We are committed to providing accessible customer service.
If you need accessible formats or communications supports, please contact us.

Nous tenons à améliorer l’accessibilité des services à la clientèle.
Si vous avez besoin de formats accessibles ou d’aide à la communication, veuillez nous contacter.

Saturday Night Project
2018 Exploration Program

August 2nd, 2019

Grant Mourre
Exploration Manager
Transition Metals Corp.

Contents

Introduction

In 2018, Transition Metals Corporation (TMC) completed exploration work programs consisting of a small ground based geophysical survey on its 100% owned Saturday Night Program. The property was staked by TMC in April 2015 to cover a prominent reversely polarized magnetic anomaly that was identified from a new aeromagnetic survey flown by the Ontario Geological Survey. In 2016, TMC completed ground based geophysical surveys (magnetics and gravity) followed by a short 601 m drill program. This work resulted in the discovery of a new PGM-Cu-Ni mineralized mafic-ultramafic intrusion called the Saturday Night Intrusion that is related to the Midcontinent Rift.

Location

The Saturday Night Project is located approximately 25 km northwest of the City of Thunder Bay, Ontario (Figure 1). Access to the Sunday Lake property is attained via Thunder Bay by travelling west on Hwy. 102 to Mapleward Road. Follow Mapleward north for 10 km where it becomes Hwy 591. Continue north for an additional 10 km where the highway transects the property. Further access can be attained through a logging road which exits west from highway 591. Project location details are summarized below:

Township: Fowler, Ware
NTS Map Sheet: 52A / 11
Latitude: 48.644210°
Longitude: -89.465576°

Land Tenure

The Saturday Night Project is comprised of 63 single cell mining claims which are summarized in Table 1 and shown on Figure 2.

Table 1: Saturday Night Claim Details

Project Name	Township / Area	Tenure ID	Tenure Type	Anniversary Date	Percentage	Work Required	Total Reserve	Legacy Claim Id
Saturday	FOWLER	108378	Single Cell Mining Claim	2023-04-16	100	$ 400	$ -	4283402
Saturday	FOWLER	108379	Single Cell Mining Claim	2023-04-16	100	$ 400	$ -	4283402
Saturday	FOWLER	108380	Single Cell Mining Claim	2023-04-16	100	$ 400	$ -	4283402
Saturday	FOWLER	108381	Single Cell Mining Claim	2023-04-16	100	$ 400	$ -	4283402
Saturday	FOWLER,WARE	108382	Single Cell Mining Claim	2023-04-16	100	$ 200	$ -	4283402
Saturday	FOWLER	108676	Single Cell Mining Claim	2020-01-17	100	$ 200	$ -	4266041
Saturday	FOWLER	108677	Single Cell Mining Claim	2023-04-16	100	$ 200	$ 2,949	4266041
Saturday	FOWLER	108678	Single Cell Mining Claim	2020-01-17	100	$ 200	$ -	4266041
Saturday	FOWLER	108679	Single Cell Mining Claim	2020-01-17	100	$ 200	$ -	4266041
Saturday	FOWLER	110077	Single Cell Mining Claim	2020-04-16	100	$ 400	$ -	4283403
Saturday	FOWLER	126783	Single Cell Mining Claim	2023-04-16	100	$ 200	$ 2,949	4283401
Saturday	FOWLER	133627	Single Cell Mining Claim	2020-01-17	100	$ 200	$ -	4266041
Saturday	FOWLER,WARE	138833	Single Cell Mining Claim	2023-04-16	100	$ 200	$ 2,749	4283401
Saturday	FOWLER,WARE	139056	Single Cell Mining Claim	2020-04-16	100	$ 200	$ -	4283403
Saturday	FOWLER	144293	Single Cell Mining Claim	2023-04-16	100	$ 400	$ -	4283402
Saturday	FOWLER	150301	Single Cell Mining Claim	2020-01-17	100	$ 200	$ -	4266041
Saturday	FOWLER	159143	Single Cell Mining Claim	2020-04-16	100	$ 400	$ -	4283403
Saturday	FOWLER	159144	Single Cell Mining Claim	2020-04-16	100	$ 400	$ -	4283403
Saturday	FOWLER	161197	Single Cell Mining Claim	2023-04-16	100	$ 200	$ 3,749	4283401
Saturday	FOWLER	161198	Single Cell Mining Claim	2023-04-16	100	$ 200	$ 3,749	4283401
Saturday	FOWLER,WARE	161199	Single Cell Mining Claim	2023-04-16	100	$ 200	$ 3,749	4283401
Saturday	FOWLER	172889	Single Cell Mining Claim	2023-04-16	100	$ 400	$ 3,749	4283401
Saturday	FOWLER	173626	Single Cell Mining Claim	2020-04-16	100	$ 400	$ -	4283403
Saturday	FOWLER,WARE	176363	Single Cell Mining Claim	2023-04-16	100	$ 200	$ 3,749	4283401
Saturday	FOWLER	190811	Single Cell Mining Claim	2023-04-16	100	$ 400	$ -	4283402
Saturday	FOWLER	191671	Single Cell Mining Claim	2020-04-16	100	$ 400	$ -	4283403
Saturday	FOWLER	195227	Single Cell Mining Claim	2023-04-16	100	$ 400	$ 3,749	4283401
Saturday	FOWLER	198424	Single Cell Mining Claim	2020-01-17	100	$ 200	$ -	4266041
Saturday	FOWLER,WARE	202961	Single Cell Mining Claim	2023-04-16	100	$ 200	$ -	4283402
Saturday	FOWLER,WARE	202962	Single Cell Mining Claim	2023-04-16	100	$ 200	$ -	4283402
Saturday	FOWLER	205763	Single Cell Mining Claim	2020-01-17	100	$ 200	$ -	4266041
Saturday	FOWLER	209610	Single Cell Mining Claim	2023-04-16	100	$ 400	$ -	4283402
Saturday	FOWLER	211149	Single Cell Mining Claim	2020-04-16	100	$ 400	$ -	4283403
Saturday	FOWLER	211150	Single Cell Mining Claim	2020-04-16	100	$ 400	$ -	4283403
Saturday	FOWLER	227504	Single Cell Mining Claim	2023-04-16	100	$ 400	$ -	4283402
Saturday	FOWLER	227505	Single Cell Mining Claim	2023-04-16	100	$ 400	$ 3,749	4283401
Saturday	FOWLER	245524	Single Cell Mining Claim	2020-01-17	100	$ 200	$ -	4266041
Saturday	FOWLER	246975	Single Cell Mining Claim	2023-04-16	100	$ 400	$ -	4283402
Saturday	FOWLER,WARE	248372	Single Cell Mining Claim	2020-04-16	100	$ 200	$ -	4283403
Saturday	FOWLER	253090	Single Cell Mining Claim	2020-01-17	100	$ 400	$ -	4266041
Saturday	FOWLER	265099	Single Cell Mining Claim	2020-01-17	100	$ 200	$ -	4266041
Saturday	FOWLER	286632	Single Cell Mining Claim	2023-04-16	100	$ 400	$ -	4283402
Saturday	FOWLER	286633	Single Cell Mining Claim	2023-04-16	100	$ 400	$ -	4283402
Saturday	FOWLER	289579	Single Cell Mining Claim	2023-04-16	100	$ 200	$ 3,749	4266041
Saturday	FOWLER	294138	Single Cell Mining Claim	2023-04-16	100	$ 400	$ 3,749	4283401
Saturday	FOWLER	301643	Single Cell Mining Claim	2020-01-17	100	$ 200	$ -	4266041
Saturday	FOWLER	306815	Single Cell Mining Claim	2023-04-16	100	$ 400	$ -	4283402
Saturday	FOWLER	306816	Single Cell Mining Claim	2023-04-16	100	$ 400	$ 149	4283401
Saturday	FOWLER	313536	Single Cell Mining Claim	2023-04-16	100	$ 400	$ -	4283402
Saturday	FOWLER	314367	Single Cell Mining Claim	2020-04-16	100	$ 400	$ -	4283403
Saturday	FOWLER	340451	Single Cell Mining Claim	2020-01-17	100	$ 200	$ -	4266041
Saturday	FOWLER	345038	Single Cell Mining Claim	2023-04-16	100	$ 400	$ -	4283402
Saturday	FOWLER	539654	Single Cell Mining Claim	2021-01-24	100	$ 400	$ -	
Saturday	FOWLER	539655	Single Cell Mining Claim	2021-01-24	100	$ 400	$ -	
Saturday	FOWLER	539656	Single Cell Mining Claim	2021-01-24	100	$ 400	$ -	
Saturday	FOWLER	539657	Single Cell Mining Claim	2021-01-24	100	$ 400	$ -	
Saturday	FOWLER	539658	Single Cell Mining Claim	2021-01-24	100	$ 400	$ -	
Saturday	FOWLER	539659	Single Cell Mining Claim	2021-01-24	100	$ 400	$ -	
Saturday	FOWLER	539660	Single Cell Mining Claim	2021-01-24	100	$ 400	$ -	
Saturday	FOWLER	539661	Single Cell Mining Claim	2021-01-24	100	$ 400	$ -	
Saturday	FOWLER	539662	Single Cell Mining Claim	2021-01-24	100	$ 400	$ -	
Saturday	FOWLER	539663	Single Cell Mining Claim	2021-01-24	100	$ 400	$ -	
Saturday	FOWLER	539664	Single Cell Mining Claim	2021-01-24	100	$ 400	$ -	

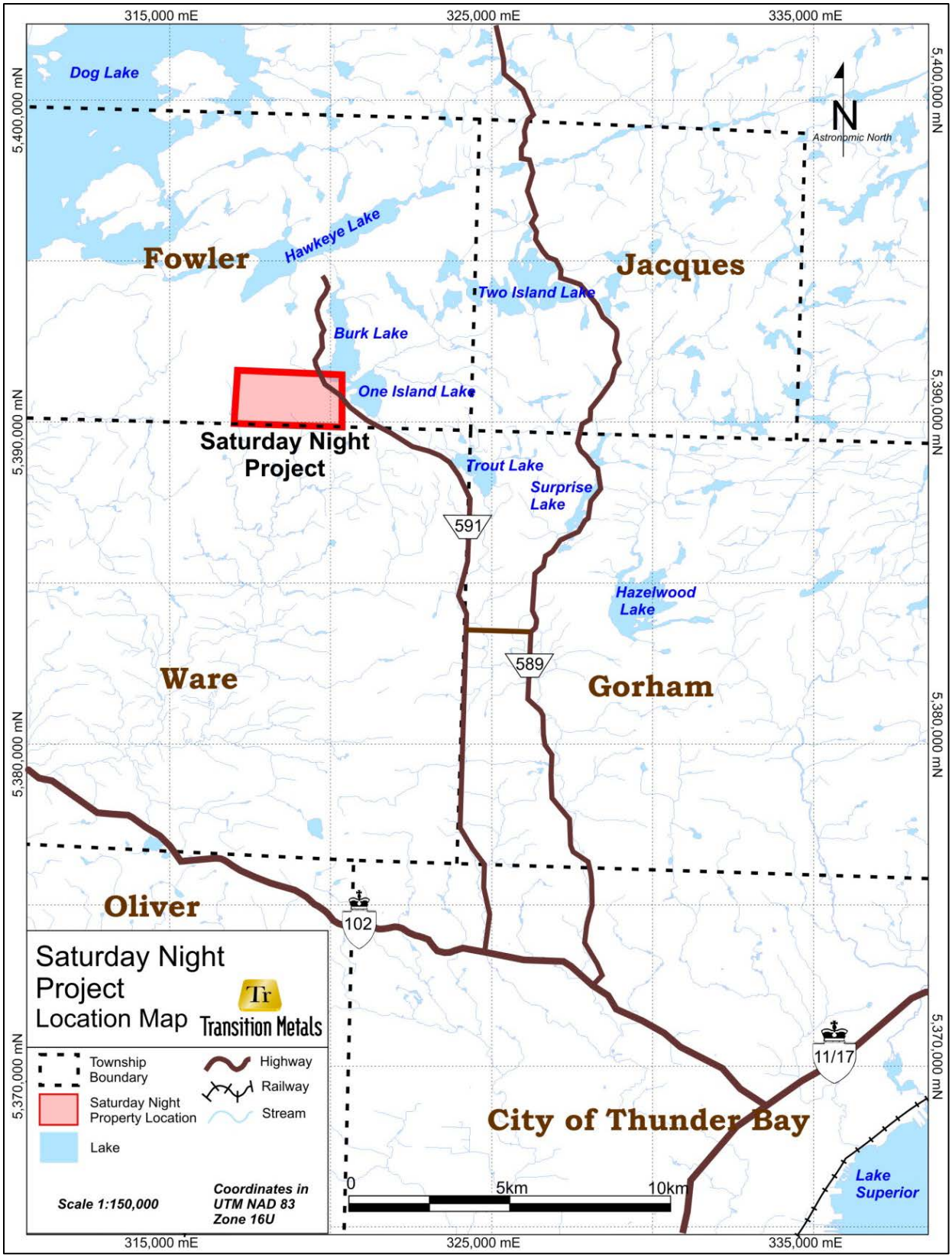

Figure 1: Saturday Night Project location map

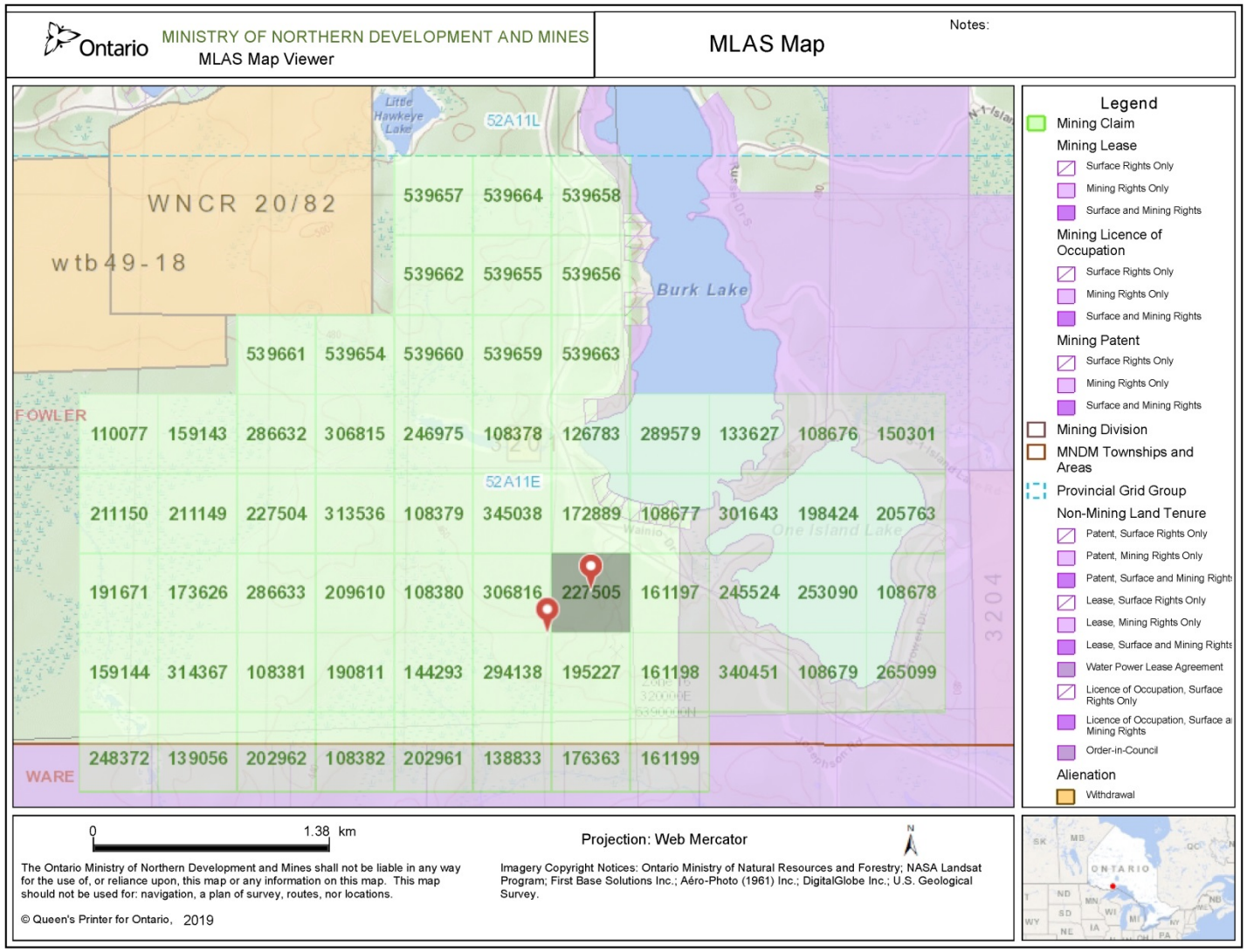

Figure 2: Saturday Night Project detailed location map

Regional Geology

The Saturday Night Project is located within the Quetico Basin of the Superior Province in Ontario and along the periphery of the Proterozoic Midcontinent Rift (MCR). Rocks of the Quetico Basin, also referred to as the Quetico Subprovince, form a 1000km, east-west trending belt that averages 70km in width stretching from Minnesota to Quebec (Williams, 1991; Stott et al. 2010). The basin is bounded to the north by the West Wabigoon, Marmion and East Wabigoon Terranes and to the south by the Wawa Terrane (Percival, 2007). Within the Quetico Basin, turbiditic metasedimentary rocks are dominant with minor iron formation, felsic intrusions, and mafic-ultramafic intrusions (Williams, 1991). These rocks are interpreted to have formed as an accretionary prism between the converging Wabigoon and Wawa Terranes (Percival, 1988). Subsequent tectonism and felsic plutonism resulted in the formation of migmatites, gneisses, and numerous suites of felsic intrusives including tonalites, granodiorites, granites, and peraluminous granites (Williams, 1991).

The Midcontinent Rift (MCR) is one of the world's largest flood basalt provinces, extending nearly 2500 km from Kansas in the southwest, arcing underneath Lake Superior and terminating at the Grenville Front in Michigan (Cannon, 1992, Figure 3). It is remotely observed as a prominent magnetic and gravity anomaly, with exposures of volcanic, sedimentary and intrusive rocks found extending from the shores of Lake Superior in Ontario, Minnesota, Wisconsin and Michigan. The vast majority of volcanic and sedimentary rocks associated with the MCR are concealed beneath Lake Superior where their thickness has been estimated at up to 30 km based on seismic reflection surveys (Cannon et al. 1989).

In the Thunder Bay region, rocks of the MCR are dominated by intrusive sills and dykes which create a landscape of mesas and ridges that define the topography of much of the region. Volcanic rocks related to the MCR are relatively minor here, confined to the Black Bay Peninsula and St. Ignace Island areas, and are known collectively as the Osler Group. The intrusive rocks surrounding the Thunder Bay area are the oldest expressions of the rift with age dates ranging from 1124-1109 Ma (Heaman et al. 2007). They are emplaced into Archean rocks of the Superior Province as well as overlying Proterozoic sedimentary rocks of the Animike and Sibley Groups. Extensive research has completed on the intrusions through the Lake Nipigon Regional Geoscience Initiative between of the Thunder Bay area which resulted in the subdivision of two broad groups of intrusions; mafic sills (Logan and Nipigon type sills) and 'early-rift' mafic to ultramafic intrusions (Hollings et al. 2007). As suggested, the 'early-rift' type intrusions predate the more extensive mafic sills as evident by age dating and observed cross-cutting relationships. The mafic sills are characterized by dominantly reversely polarized magnetic signatures while the 'early-rift' intrusions have both reversely and normally polarized magnetic signatures.

Exploration of MCR related intrusions has persisted for decades within the Duluth Complex, the Great Lakes Nickel Deposit and the Coldwell Complex (Marathon deposit) focusing largely on the base metal potential of these large tonnage, low grade deposits. As the geological understanding of the MCR became better understood, researchers recognized the potential for world class Ni-Cu-PGM deposits similar to those hosted in the analogous Norilsk mining camp of Russia. This information, coupled with rising precious metal prices in the late 1990's – early 2000's spurred a flurry of exploration activity in the

region which ultimately led to new discoveries in Michigan (Eagle Mine), Minnesota (Tamarack deposit) and in Ontario (Thunder Bay North Deposit).

Unlike the large tonnage, low grade deposits previously discovered, these new discoveries boasted high grade Ni-Cu dominated mineralization at Eagle and Tamarack, and high grade PGM dominated mineralization at Thunder Bay North. These deposits are all hosted within 'early-rift' type irregularly shaped, primitive, ultramafic to mafic intrusions interpreted to be feeders or chonoliths within a more extensive magmatic system.

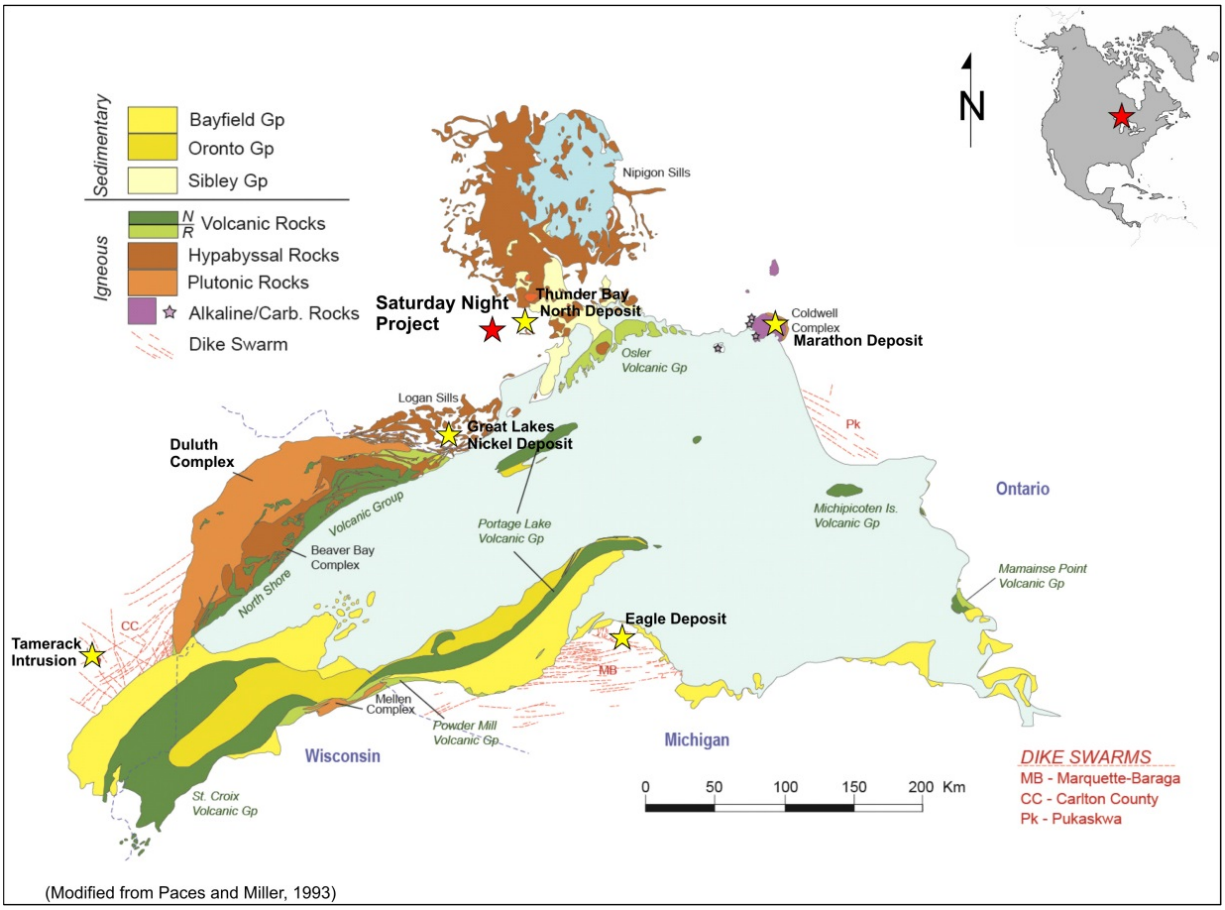

Figure 3: Geology of the Midcontinent Rift with notable mineral deposits and intrusions.

Local Geology

The bedrock geology of the Saturday Night property is compiled from 1:250,000 scale mapping by the Ontario Geological Survey, shown on Figure 4a. As mapped, the project area is dominated by granite-granodiorite with thin veneers of Quetico metasedimentary rocks to the north and south west. Although the mapped granitic units appear to be laterally extensive, recent work has identified a discreet assemblage of magnetite bearing granites, termed the Dog Lake Granite Chain, which are distinct from the granite-granodiorite suite described in the OGS map (Kuzmich et al. 2012). In particular the property appears to cover the northern margin of the Trout Lake Granite, a post-tectonic

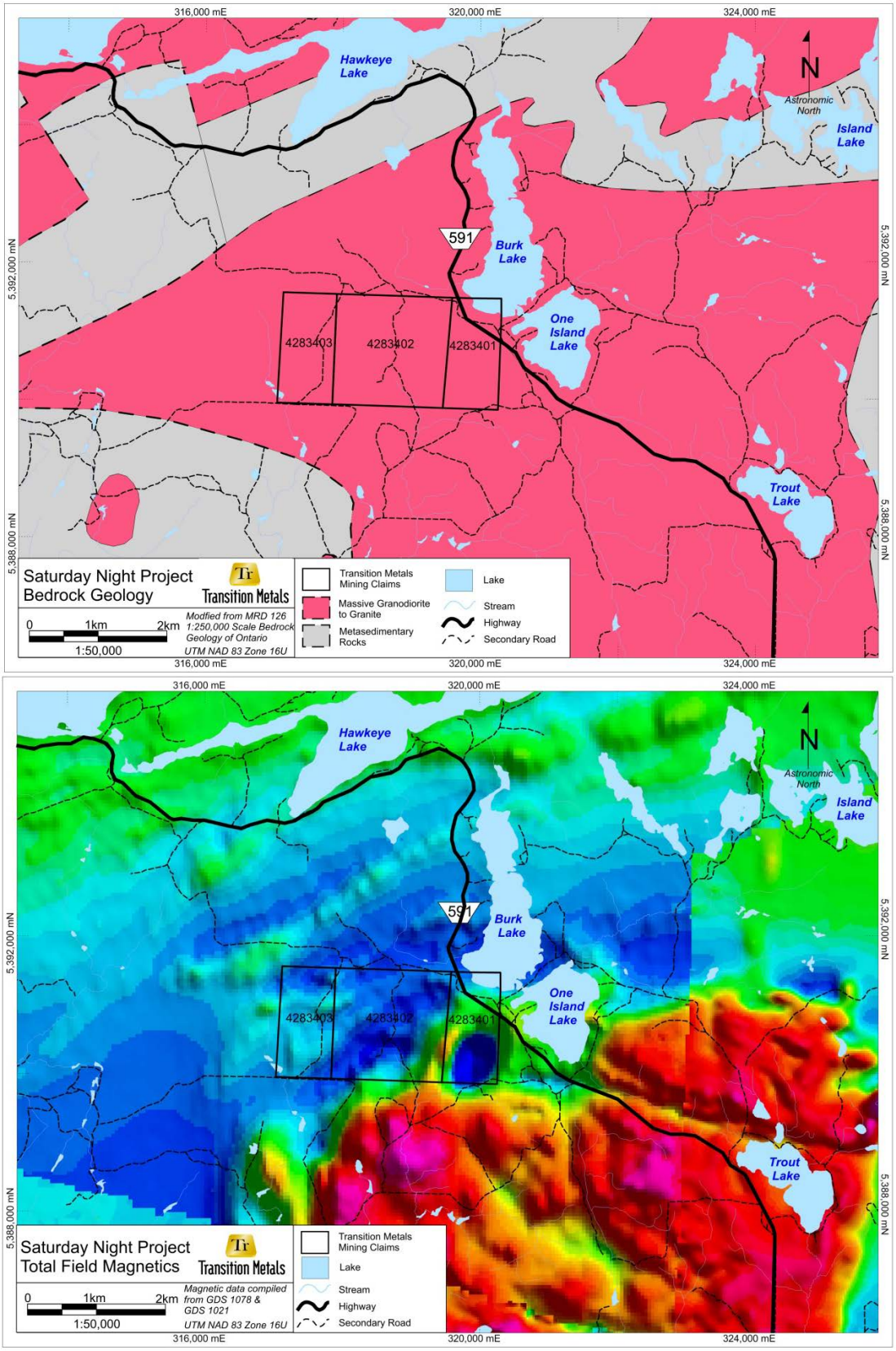

Figure 4: a) Bedrock Geology of the Saturday Night property. b) Total field magnetics of the Saturday Night property

I-Type granite. This observation is reinforced by publically available aeromagnetic data which show a discreet circular magnetic high which stands apart from the regional northeast trending magnetic fabric (Figure 4b).

The bedrock geology directly underlying the Saturday Night property is obscured by thick accumulations of glacial sediments. A major glacial feature, the Dog Lake Moraine, extends across the property as shown in Figure 5. Because of the thick overburden cover, a bedrock source for the Saturday Night magnetic anomaly has yet to be identified and the local bedrock geology must be inferred from remote geophysical techniques.

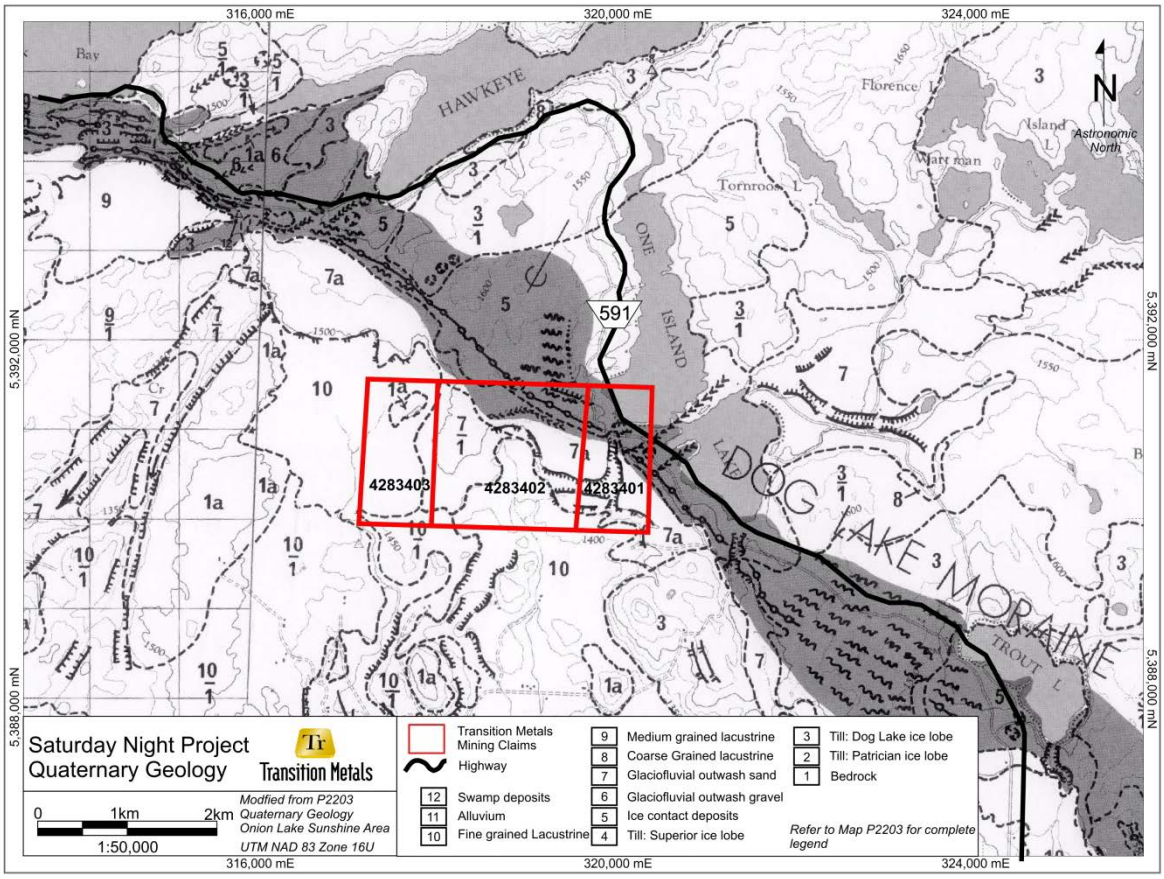

Figure 5: Quaternary geology of the Saturday Night property

Exploration Target

The Saturday Night Project is considered to be highly prospective for MCR related magmatic Ni-Cu-PGM mineralization, similarities to other mineralized MCR intrusions in the area such as the Thunder Bay North Deposit (9.83 Mt @ 2.87 g/t Pt-Eq for 0.741 Moz Pt-Eq (Indicated) + 0.53 Mt @ 2.87 g/t Pt-Eq for 0.05 Moz Pt-Eq (Inferred)) and the Sunday Lake Intrusion (41.2 m @ 5.51 g/t PGM, 0.57 % Cu, 0.19 % Ni). These projects are characterized by prominent roughly circular reversely polarized magnetic signatures and are situated along contacts between granitic and metasedimentary rocks (Figure 6).

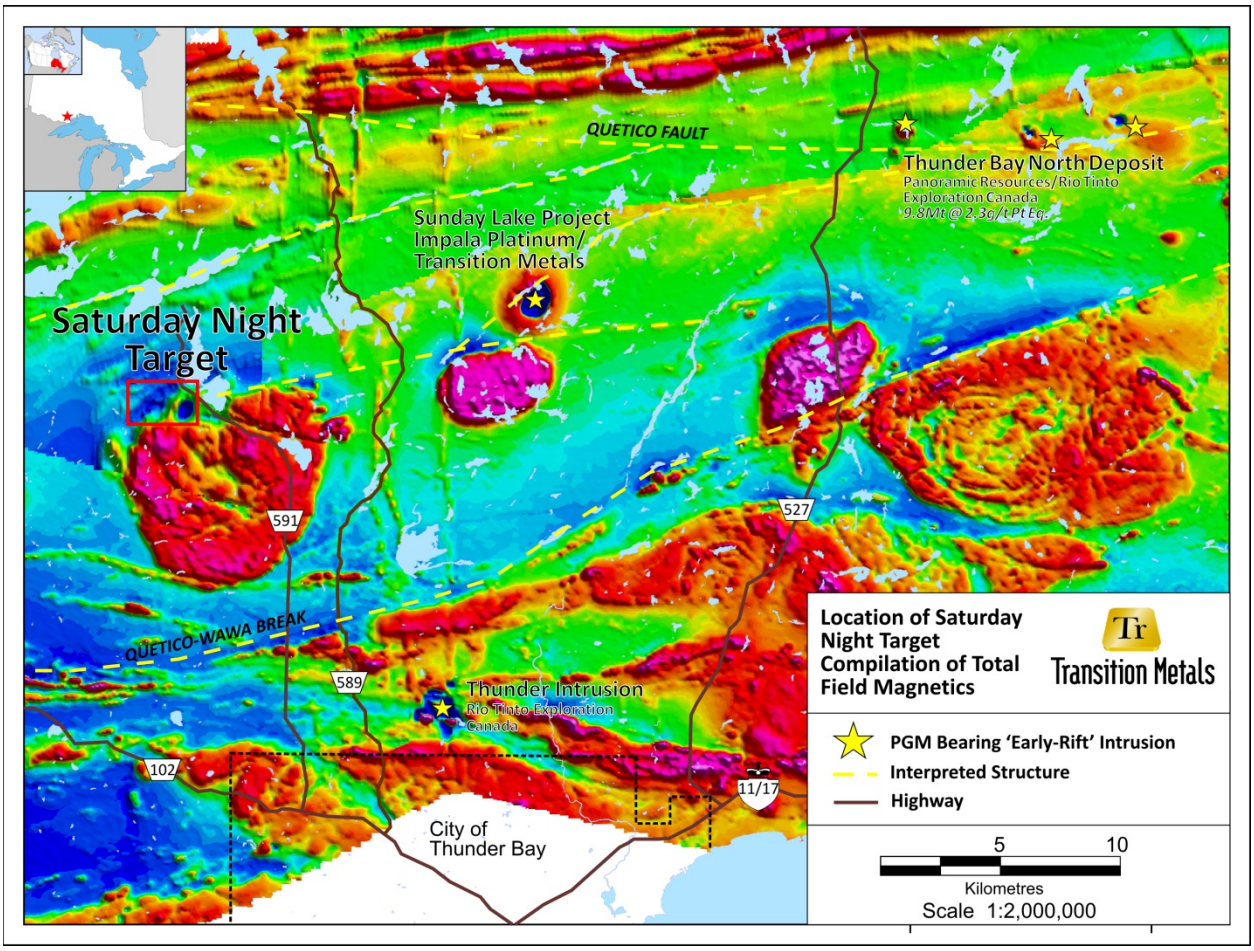

Figure 6: Regional magnetic signature of the Thunder Bay area

The Saturday Night magnetic anomaly is roughly circular and approximately 1 km in diameter and sits along the northern margin of the Trout Lake granite. With no bedrock exposure present atop the Saturday Night magnetic anomaly, exploration must be conducted using a combination of geophysics and diamond drilling.

Previous Work

2016: Transition Metals completed regional prospecting, a ground magnetics survey (15 km), ground gravity survey (71 gravity stations) and completed a single 601 m drill hole to test the magnetic anomaly.

2018 Exploration Program

Ground Geophysics

EMPulse Geophysics Ltd., based out of Dalmeny, Saskatchewan, was contracted to complete a ground based PULSAR Magnetotellurics (MT) Survey across a portion of the Saturday Night Property. A total of 34 stations at approximately 200 m spacings were collected on six roughly parallel lines over the target area (Figure 7). Work was completed between August 4th and August 12th. The complete geophysical report is included in Appendix A.

The completed MT was completed without the use of cut grid lines or a designated power source such as a generator. As a result no NMDM approved exploration plans or permits were required.

Sample stations 6, 12, 19, 25 and 32 were collected off of Transition Metals Saturday Night Property and as a result expenses associated with the collect of that data was subtracted from the total (see Table 2).

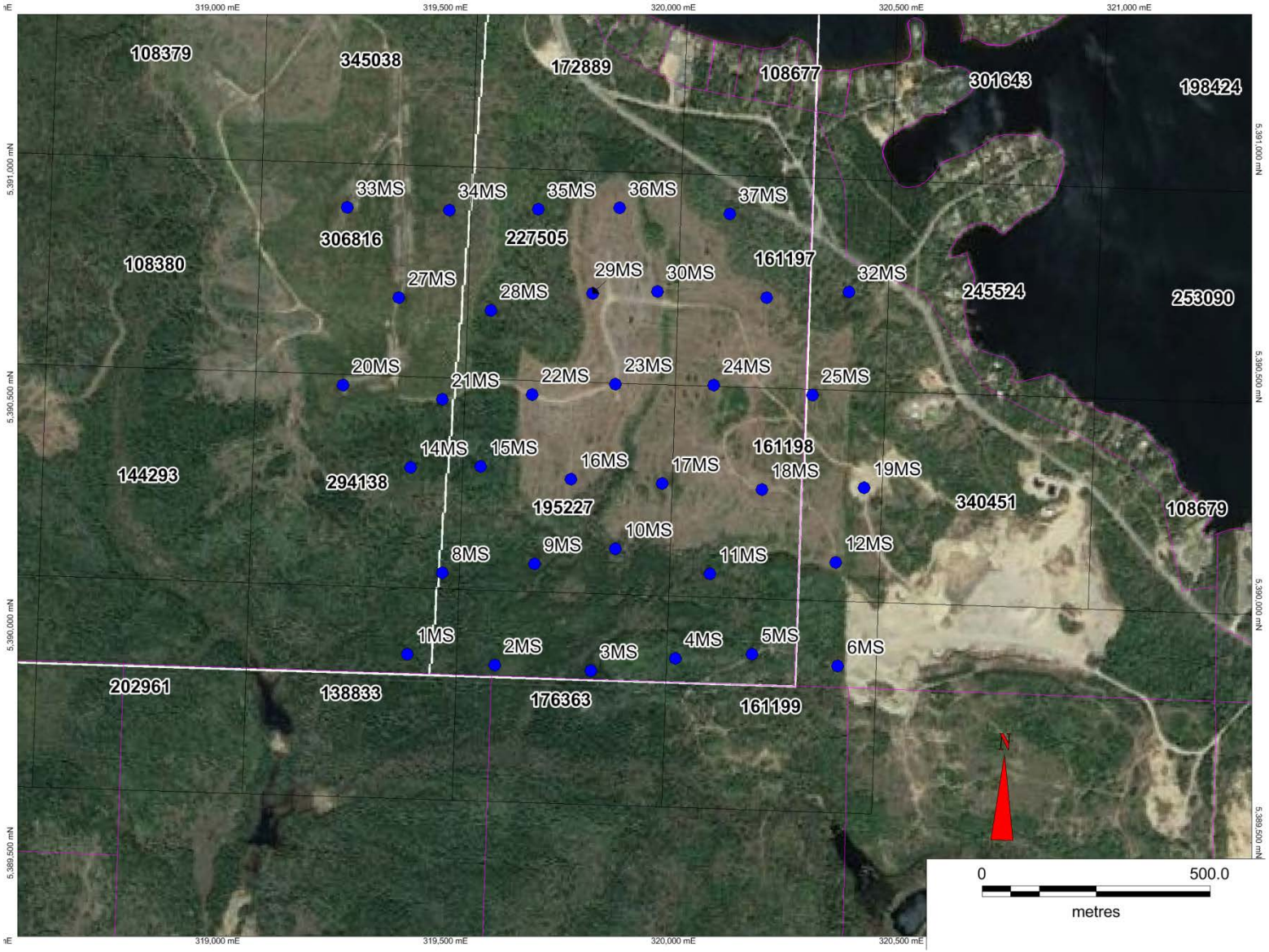

Figure 7: Map showing the location of the 2018 MT survey stations.

Results and Conclusions

The MT survey completed at the Saturday Night Project has revealed that the Saturday Night Intrusion extends much further than originally interpreted based on the ground magnetics. Furthermore, the results from the MT survey suggest a complex morphology to the basal contact that includes potential traps for sulphide mineralization such as is seen at the nearby Sunday Lake Intrusion.

Expenditures

The table below summarizes the expenditures incurred during exploration activities at Saturday Night. Expenditure details, including receipts and proof of payment are included in Appendix B.

Table 2: 2018 Saturday Night Project expenditure summary table.

Exploration Activity	**Units**	**Actual Cost**
Magnetotelluric Survey		
EMpulse - Invoice 18-03		$8,400.00
EMpulse - Invoice 18-04		$15,400.00
EMpulse - Invoice 19-02		$11,700.00
Total (34 station)		$35,500.00
Cost per station		$1,044.12
Station Reduction (6,12,19,25,32)		$5,220.59
Total amount claimed (29 stn)		**$30,279.41**
Claim Number	Stations	Actual Cost
161199 (minus stn 6 – off of property)	2	$2,088.23
176363	2	$2,088.23
138833	1	$1,044.12
161198 (minus stn 12,19,25 – off of property)	2	$2,088.24
195227	7	$7,308.83
294138	3	$3,132.35
161197 (minus stn 32 – off of property)	3	$3,132.35
227505	6	$6,264.71
306816	3	$3,132.35
Total	**29**	**$30,279.41**

Signature

Grant Mourre, P.Geo
19 Kristi Court
Sudbury ON, CANADA
P3E 5R4

I, Grant Mourre, do hereby certify that:

1. I am employed as an Exploration Manager for Transition Metals Corporation a publically traded mineral exploration company.
2. I have been granted the degrees of Master of Science in Geology from Laurentian University, Sudbury, Ontario (2000) and Honours Bachelor of Science Degree in Geology from the University of Saskatchewan, Saskatoon, Saskatchewan (1997).
3. I am a Practising Member in good standing of the Association of Professional Geoscientists of Ontario (APGO member #0566).
4. I have worked as an exploration geologist in Canada for over 20 years.
5. I did personally conduct exploration activities on the Saturday Night Property during 2018.

Dated the 1st day of August, 2019

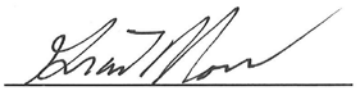

Grant Mourre, P. Geo.

References

Cannon, W., Green, A., Hutchinson, D., Lee, M., Milkereit, B., Behrendt, J., Halls, H., Green, J., Dickas, A., Morey, G., Sutcliffe, R., and Spencer, C., 1989. The North American Midcontinent Rift beneath Lake Superior from GLIMPCE seismic reflection profiling. Tectonics. v.8, p305–332

Cannon, W. F., 1992. The Midcontinent rift in the Lake Superior region with emphasis on its geodynamic evolution. Tectonophysics. v.213, p41-48

Davis, D.W., Pezzuto, F., and Ojakangas, R.W., 1990. The age and provenance of metasedimentary rocks in the Quetico subprovince, Ontario, from single zircon analyses: Implications for Archean sedimentation and tectonics in the Superior Province: Earth and Planetary Science Letters, v. 99, p. 195-205.

Heaman, L. M., Easton, R. M., Hart, T. R., Hollings, P., MacDonald, C. A., and Smyk, M., 2007. Further refinement to the timing of Mesoproterozoic magmatism, Lake Nipigon region, Ontario. Canadian Journal of Earth Sciences v. 44, p. 1055-1086

Hollings, P., Hart, T. R., Richardson, A., MacDonald, C. A., 2007. Geochemistry of the Mesoproterozoic intrusive rocks of the Nipigon Embayment, northwestern Ontario: evaluating the earliest phases of rift development. Canadian Journal of Earth Sciences. v. 44, p. 1087-1110

Kuzmich, B., Hollings, P., Scott, J. F., Campbell, D. A., 2011. Geochemistry and Petrology of the Dog Lake Granite Chain, Quetico Subprovince, Thunder Bay: A Preliminary Report, *in* Summary of Field Work and Other Activities 2011, Ontario Geological Survey, Open File Report 6270, p.8-1 to 8-8

Percival, J.A., 1988. A regional perspective of the Quetico metasedimentary belt, Superior Province, Canada: Canadian Journal of Earth Sciences, v.26, p. 677-693

Percival, J.A., 2007. Geology and metallogeny of the Superior Province, Canada. In: Goodfellow,W.D. (Ed.), Mineral Deposits of Canada: A Synthesis of Major Deposit-Types, District Metallogeny, the Evolution of Geological Provinces, and Exploration Methods: Geological Association of Canada, Mineral Deposits Division, Special Publication No. 5, p. 903-928

Stott, G.M., Corkery, M.T., Percival, J.A., Simard, M., and Goutier, J., 2010. A revised Terrane Subdivision of the Superior Province, *in* Summary of Field Work and Other Activities, Ontario Geological Survey, Open File Report 6260, p.20-1 to 20-10

Williams, H. R. 1991. Quetico Subprovince, *in* Geology of Ontario, Ontario Geological Survey, Special v 4, Part I, p383-403

Appendix A

Saturday Night Project: PULSAR Survey Results

David K. Goldak, M.Sc., P.Eng.

Abstract

A PULSAR survey was conducted by EMpulse Geophysics Ltd. approximately 25 km NW of Thunder Bay, Ontario on behalf of Transition Metals Corporation. Thirty-four stations at approximately 200 m spacing were collected on six parallel E-W lines over a mafic intrusive body within the Fowler/Ware townships.

Three-dimensional joint inversion of the impedance phase-tensor, tipper and horizontal magnetic transfer function reveals a resistive inner "core" while phase tensor inversion alone gives more so the impression of a resistive "finger" trending NW-SE.

The resistive "finger" lies in the same orientation as a clear break in the total field magnetics data which may indicate the location of large scale fault structure trending NW-SE.

This structure appears to mark the defining line along which the structural character of the intrusive body changes from "bowl" like to rectangular or "channel" like.

Near the West end L3/L4, a large vertical offset is seen within the intrusive body, implying the presence of fault structure with signifcant throw. This area of the grid also corresponds to a clear change in orientation of the resistive "finger". Weak to moderately conductive material is present within and near the bottom of the "channel" at approximately 600 m depth, the vertical offset is approximately 300 m West of DDH SN-16-001.

A much stronger resistivity low is seen at the South-West edge of the grid, within the "bowl" structural regime and may represent a footwall depression target, at approximately 1000 m depth.

Contents

List of Figures

1 Introduction

The magnetotelluric (MT) method is a geophysical exploration technique in which the earth's electrical structure at depth may be estimated from surface measurements of naturally occurring fluctuations in the earth's geomagnetic field along with electric field fluctuations induced within the earth by the former.

The chief source of naturally occurring energy in the ELF/VLF [1] bandwidth is due to lightning discharges (Pierce, 1977. Volland, 1982). Thunderstorm activity on a near global scale produces a low level, quasi-continuous component, superimposed on which, are *individual* transients which arise from either relatively nearby and/or very large current-moment lightning discharges (Tzanis and Beamish, 1987. Jones and Kemp, 1971). Note that nearby is defined relative to global waveguide attenuation. For example, nearby at 100 Hz may be 6 Mm [2] whereas at 5 kHz, perhaps 2 Mm.

Both energy sources can be used to estimate earth response curves, but as shown in Figure 1, substantial increases in signal-to-noise ratio (SNR) are afforded by recording the transient component in a time localized fashion. In so doing, the sometimes lengthy periods of relative inactivity between individual transient events are avoided, especially important in times of low source field activity, i.e., winter recordings and/or those at high latitude.

This is contrasted with conventional AMT where data is recorded continuously for some period of time under the assumption that there is a continuous influx of energy. While the continuing component is appreciable in certain frequency ranges, most notably for $f \leq 200$ Hz, the largest naturally occurring signals in the audio bandwidth are transients and are thus time localized phenomena.

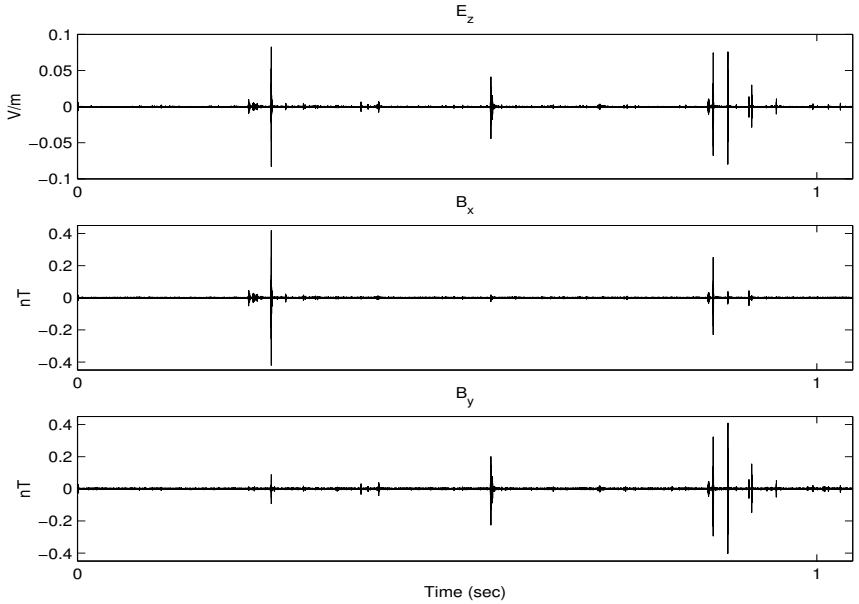

Figure 1: A typical VLF recording, Oct 18, 2001

[1] ELF: Extremely-Low Frequency, 3 Hz - 3 kHz; VLF: Very-Low Frequency, 3 kHz - 30 kHz.
[2] 1 $Mm = 1000$ km.

Therefore, PULSAR, designed and constructed by EMpulse Geophysics Ltd., obtains the best possible SNR by capturing only transient energy in the 1 Hz - 40 kHz bandwidth through simple amplitude triggering and subsequent time localized recording. We have furthermore developed a data processing algorithm which properly incorporates the polarization properties of the source field and SNR to obtain solid parameter and error estimates (Goldak et al., 2001).

This is superior to conventional AMT data processing (Remote-Reference) which assumes a circularly polarized source field (signals arriving from all directions), infinite sample size and makes assumptions about the statistical distribution of the noise (Gamble et al., 1979).

Our Adaptive Polarization Stacking (APS) algorithm makes no such assumptions and is thus better connected with the real properties of the data (polarization, sample size, SNR) resulting in well estimated parameters and errors. We have also shown that, given typical polarization characteristics of transient data, our APS algorithm has a higher order bias convergence than Remote-Reference (Goldak et al., 2001).

The fundamental quantity of interest for MT surveys is the impedance tensor $\tilde{\mathbf{Z}}$ which is the transfer function between mutually orthogonal, horizontal components of magnetic and electric fields as defined in equation (1). Implicit in the definition of the impedance tensor is that we work in the frequency domain, with a right handed co-ordinate system typically defined with ^{+}x North, ^{+}y East and ^{+}z down.

$$\begin{bmatrix} \tilde{E}_x \\ \tilde{E}_y \end{bmatrix} = \begin{bmatrix} \tilde{Z}_{xx} & \tilde{Z}_{xy} \\ \tilde{Z}_{yx} & \tilde{Z}_{yy} \end{bmatrix} \cdot \begin{bmatrix} \tilde{H}_x \\ \tilde{H}_y \end{bmatrix} \tag{1}$$

or simply

$$\tilde{\mathbf{E}} = \tilde{\mathbf{Z}}\tilde{\mathbf{H}}.$$

Another quantity of interest is the magnetic field tipper $\tilde{\mathbf{T}}$ which relates horizontal and vertical magnetic field components, as defined in equation (2).

$$\tilde{H}_z = \tilde{T}_x\tilde{H}_x + \tilde{T}_y\tilde{H}_y. \tag{2}$$

The name "tipper" refers to the tipping or tilting of the total magnetic field in the vicinity of lateral conductivity changes due to disruption in sub-surface current flow. The tipper is therefore very useful for locating discrete features and for assessing data dimensionality. For example, in a one-dimensional earth there exists no vertical magnetic field of secondary origin and thus the tipper $\tilde{\mathbf{T}}$ vanishes.

Tipper data is essentially like classical VLF data with two very important distinctions. Firstly, the tipper is measured across a much wider bandwidth (1 Hz - 40 kHz) giving a much greater depth of penetration and conductance aperture. Secondly, the tipper measurement is tensor, which means that we observe the response with electromagnetic waves arriving from many different directions.

VLF data is essentially single frequency and because the transmitter is in one fixed orientation with local geology, coupling issues may arise. Therefore, the tipper allows us to observe VLF like responses from very deep (and shallow) conductors, across a much wider range of conductance (with less saturation), and also removes coupling issues due to the tensor measurement.

In the one-dimensional isotropic case the tipper vanishes and the impedance tensor takes on a very simple form as shown in equation (3).

$$\begin{bmatrix} 0 & \tilde{Z}_\circ \\ -\tilde{Z}_\circ & 0 \end{bmatrix} \tag{3}$$

We see that the modulus of $\tilde{\mathbf{Z}}$ (apparent resistivity ρ) is singly valued and the argument of the two non zero components of $\tilde{\mathbf{Z}}$ (phase ϕ) are simply shifted by π radians. Of course in the 1D anisotropic case the modulus of $\tilde{\mathbf{Z}}$ is no longer singly valued. The only way to distinguish a 1D anisotropic earth from a two-dimensional earth is through measurement of $\tilde{\mathbf{T}}$.

If earth resistivity structure is two-dimensional and the co-ordinate system is aligned with strike, the diagonal elements of $\tilde{\mathbf{Z}}$ also vanish as shown below, although the tensor is no longer singly valued.

$$\begin{bmatrix} 0 & \tilde{Z}_1 \\ \tilde{Z}_2 & 0 \end{bmatrix} \tag{4}$$

In the two-dimensional case, with the x co-ordinate axis aligned with strike, the tipper takes on a very simple form as shown below in equation (5).

$$\tilde{H}_z = \tilde{T}_y \tilde{H}_y. \tag{5}$$

The x-component of the tipper, indicative of conductive structure parallel to line, vanishes in the 2D aligned case and only the y-component remains. In the 2D unaligned case, there is a clear angle which will allow the x-component to be minimized while maximizing the y-component. In the 3D case, both the x and y components are non-zero no matter what rotation angle is used.

With finite SNR and earth structure that is typically only approximately 1D or 2D, we relax this condition and say that we are in a 1D or 2D aligned situation when the diagonal elements of $\tilde{\mathbf{Z}}$ are much smaller than the off diagonal elements. Similarly, for the tipper in the 2D aligned case, one of the T_x or T_y components should be small and mostly featureless compared to the other.

However, the Saturday Night data displays 3D character at many sites, especially for frequencies below $\approx 1\ kHz$. An example is shown in Figure 2 where we note the appreciable size of ρ_{xx} and ρ_{yy}, especially below about $1\ kHz$.

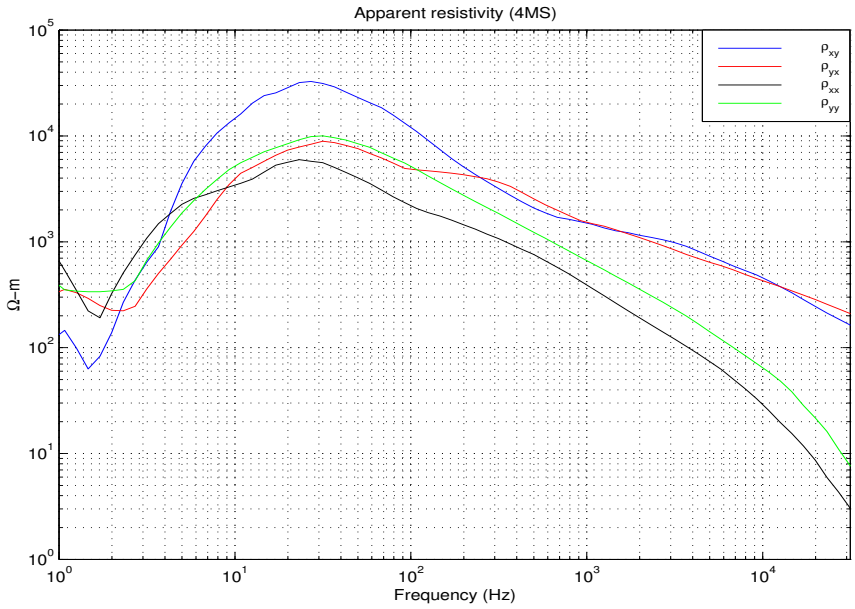

Figure 2: 3D Apparent Resistivity

For presentation purposes, earth response curves are interpolated where needed to better approximate the true response, this process is illustrated in Figure 3. Note that data errors are not interpolated, therefore, editing of the curves is unlikely to affect the final inverted model as error bars will be very large in the edited regions of the curves.

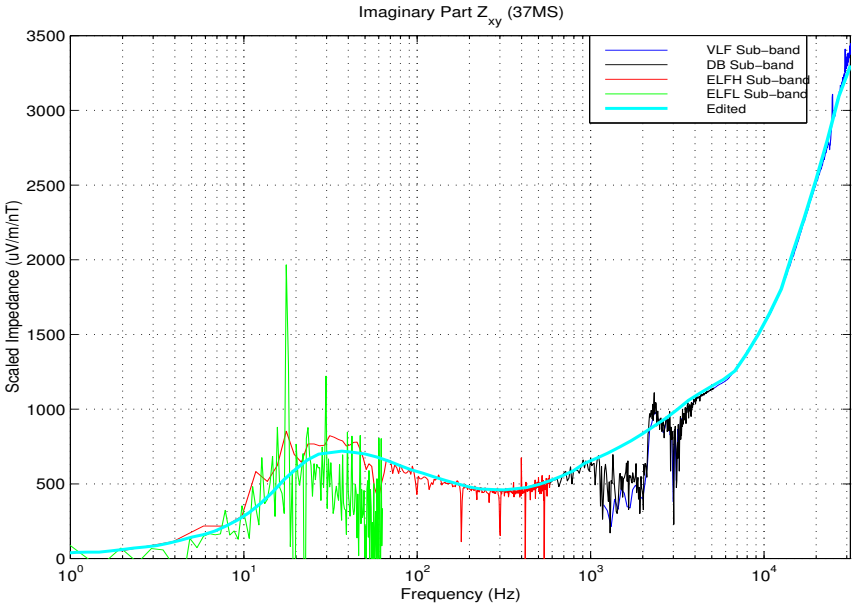

Figure 3: Edited $\tilde{Z}_{xy}$

A relatively new development in the interpretation of MT data is the impedance phase tensor (Caldwell et al., 2004). Formed by the ratio of imaginary and real parts of the impedance tensor, it is a static free quantity and has been found to be extremely useful in general 3D environments, especially when jointly inverted with the tipper (Tietze et al., 2015). If we consider $\tilde{\mathbf{X}}$ to contain the real parts of $\tilde{\mathbf{Z}}$ and $\tilde{\mathbf{Y}}$ the imaginary parts of $\tilde{\mathbf{Z}}$, the phase tensor is simply,

$$\tilde{\Phi} = \tilde{\mathbf{X}}^{-1}\tilde{\mathbf{Y}} = \begin{bmatrix} \tilde{\Phi}_{xx} & \tilde{\Phi}_{xy} \\ \tilde{\Phi}_{yx} & \tilde{\Phi}_{yy} \end{bmatrix} \tag{6}$$

As a result, the phase tensor collapses the four complex values of $\tilde{\mathbf{Z}}$ into four pure real numbers $\tilde{\Phi}$. The "primary" components $\tilde{\Phi}_{xx}$ and $\tilde{\Phi}_{yy}$ are seen to be near unity and the "secondary" components $\tilde{\Phi}_{xy}$ and $\tilde{\Phi}_{yx}$ near zero, unless anomalous conditions are present, as shown in Figure 4.

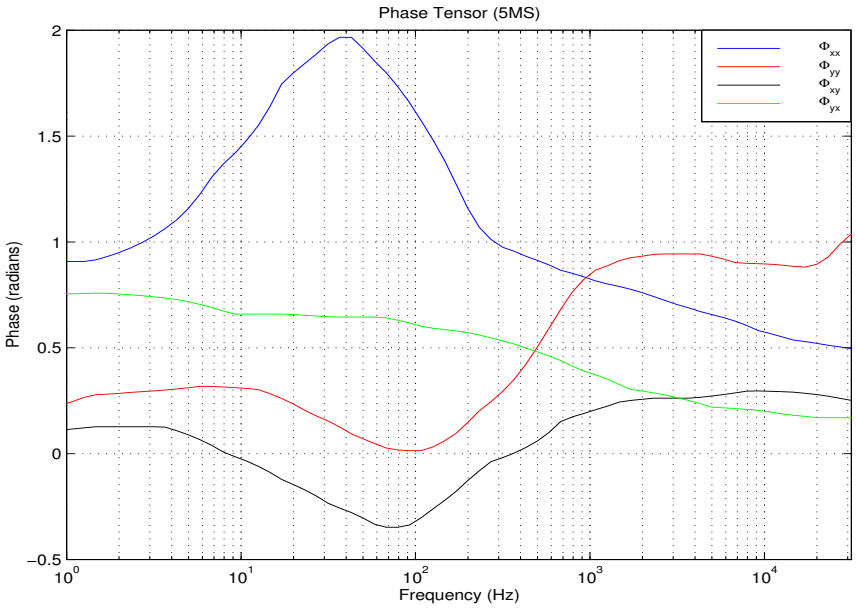

Figure 4: Anomalous Phase Tensor

The horizontal magnetic tensor $\tilde{\mathbf{M}}$ (Berdichevsky, 1968), or horizontal magnetic transfer function (MTF), is the transfer function between horizontal components of the magnetic field at a base station $\tilde{\mathbf{H}}_\mathbf{b}$, ideally located in a background environment far away from any anomalous sources, and those recorded simultaneously at some remote (possibly anomalous) station $\tilde{\mathbf{H}}_\mathbf{r}$. Note that like the impedance phase tensor and tipper, horizontal MTF's are also static free quantities.

$$\begin{bmatrix} \tilde{H}_{xr} \\ \tilde{H}_{yr} \end{bmatrix} = \begin{bmatrix} \tilde{M}_{xx} & \tilde{M}_{xy} \\ \tilde{M}_{yx} & \tilde{M}_{yy} \end{bmatrix} \cdot \begin{bmatrix} \tilde{H}_{xb} \\ \tilde{H}_{yb} \end{bmatrix} \tag{7}$$

or simply

$$\tilde{\mathbf{H}}_\mathbf{r} = \tilde{\mathbf{M}}\tilde{\mathbf{H}}_\mathbf{b}$$

The horizontal MTF's therefore indicate the uniformity of the horizontal magnetic field between the base and some remote station. In the absence of local conductivity anomalies, the remote and base fields should be in phase and show no amplitude variation or inter-dependencies. Therefore, the $\tilde{M}_{xx}$ and $\tilde{M}_{yy}$ components should be near unity amplitude and zero phase, except in locally anomalous conditions. Furthermore, the $\tilde{M}_{xy}$ and $\tilde{M}_{yx}$ components should be mostly small and featureless, except in locally anomalous conditions that are additionally off-strike with respect to our measurement co-ordinate system.

An example MTF is shown below in Figure 5, which responds strongly to the intrusive body on the Saturday Night property.

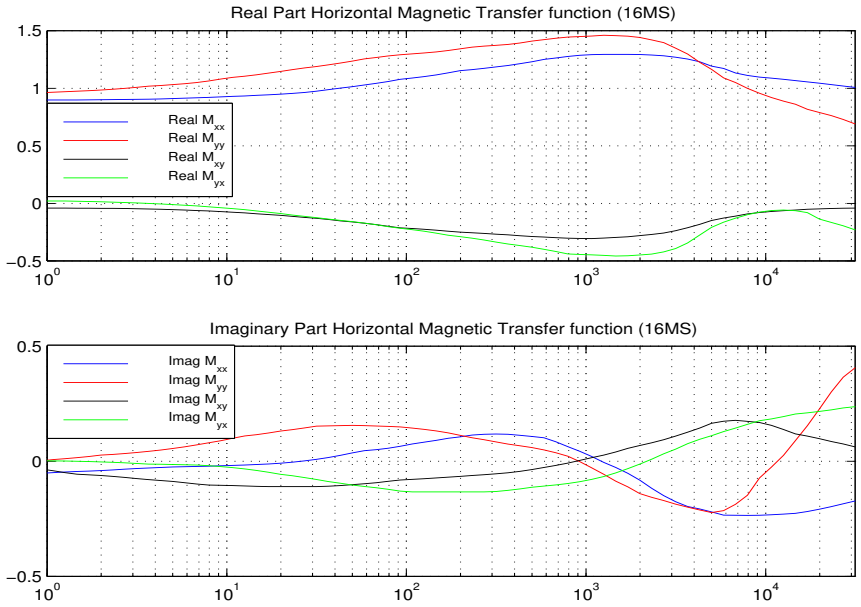

Figure 5: Example MTF

An assessment of topographic distortion was not carried out for the Saturday Night data-set. Topographic relief on the property was quite mild with generally less than 20 m elevation differences between adjacent stations.

Lastly, the interpolated data need to be "inverted" to estimate earth resistivity as a function of depth. In the 1D noise free case, the inversion is unique. However, in the 2D and 3D cases the inverse process is always non-unique, noise free data or not. Therefore, we require a means of addressing the non-uniqueness inherent to these cases. A very useful approach is embodied in the OCCAM inversion of deGroot-Hedlin and Constable (1990). Although quite slow, the OCCAM approach is conservative in that not only do we fit the data to within a prescribed tolerance, we do so in the most featureless way. In this manner, we address the issues of non-uniqueness and data fit simultaneously.

The 3D inversion code used for this project is based on the serial version of WSINV3DMT (Siripunvaraporn et al., 2005), which like the 2D OCCAM code, is also a minimum structure inversion program. Through funding from EMpulse Geophysics Ltd., WSINV3DMT was extended to include the tipper as well for full 3D inversion of both $\tilde{\mathbf{Z}}$ and $\tilde{\mathbf{T}}$. WSINV3DMT was subsequently parallelized by Peter Kosteniuk within a 64 bit Linux

environment. Thirty-two bit memory limitations have thus been overcome and due to the use of 32 CPU cores, as many as 400 stations can now be inverted in three-dimensions in a reasonable time.

Recently, Peter Kosteniuk has additionally extended our parallel version of WSINV3D so as to be able to invert the impedance phase tensor and horizontal magnetic transfer functions.

2 Data Quality Assessment

The main challenge with respect to data quality on the Saturday Night grid is due to a moderate sized powerline that parallels Gilbride Road, supplying power to many cabins on the nearby lake (Figure 6, Figure 7) and also extending North to Dog Lake[3].

With our PULSAR prototype used for this survey, no high gain analog section was present, only a high resolution, time synchronized analog-to-digital converter. Therefore, all the data (powerline noise plus signals) are recorded without clipping (distorting), the noise is then removed at home office with our adaptive powerline noise cancellation software, isolating transient signals of interest.

Example PULSAR data at station 15MS is shown in Figure 8, ≈ 1 km West of Gilbride Road, before and after noise cancellation[4]. Although the powerline that parallels Gilbride Road is much smaller than those seen at Aer-Kidd, cultural noise levels at Saturday Night are, oddly, still very high. Even and odd harmonics of 60 Hz were cancelled up to the 52'nd harmonic (3120 Hz). The effectiveness of the adaptive powerline noise cancellation filter is evident by the fine scale correlation seen between corresponding electric and magnetic fields.

After powerline noise cancellation, quality of earth response curves is good with only small to moderate dead-band effects. The capacitive line antenna functioned extremely well, high quality impedance curves, right up 40 kHz, were obtained, although contact resistance effects were not as extreme for Saturday Night as compared to Aer-Kidd.

Induction coil installations were generally quite good, except in areas of thick bush and/or swampy ground, as occurs in the SW area of the grid. Note the motion noise on H_z, shown in Figure 8.

In accord with the geomagnetic convention, co-ordinate axes were chosen as ^{+}x to the North, ^{+}y perpendicular to the East and ^{+}z vertically down.

[3]Note that stations NOT collected in Figure 7 have no numeric label.

[4]Note that the vertical scale on the lower cleaned plot is many times smaller.

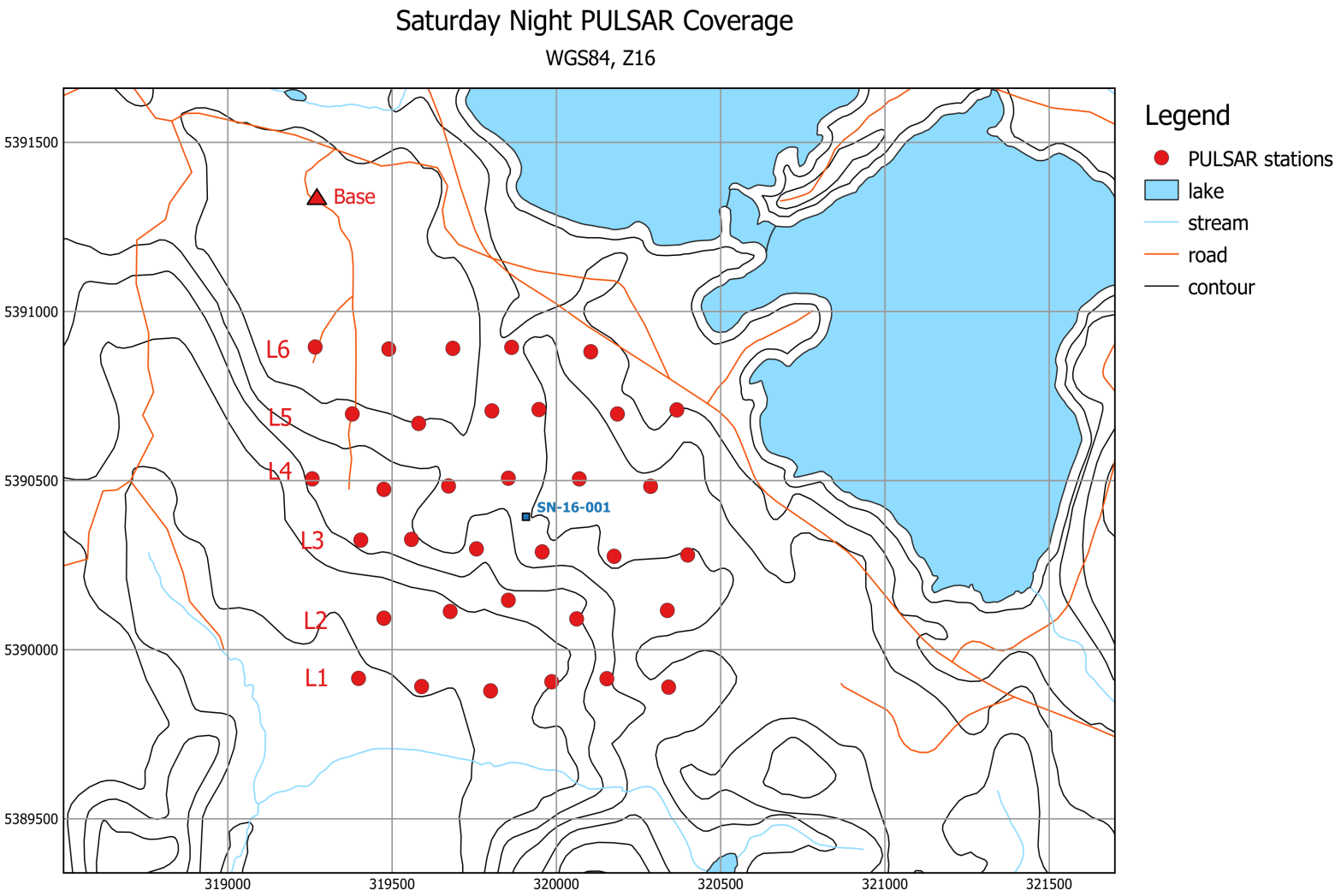

Figure 6: Saturday Night Topography

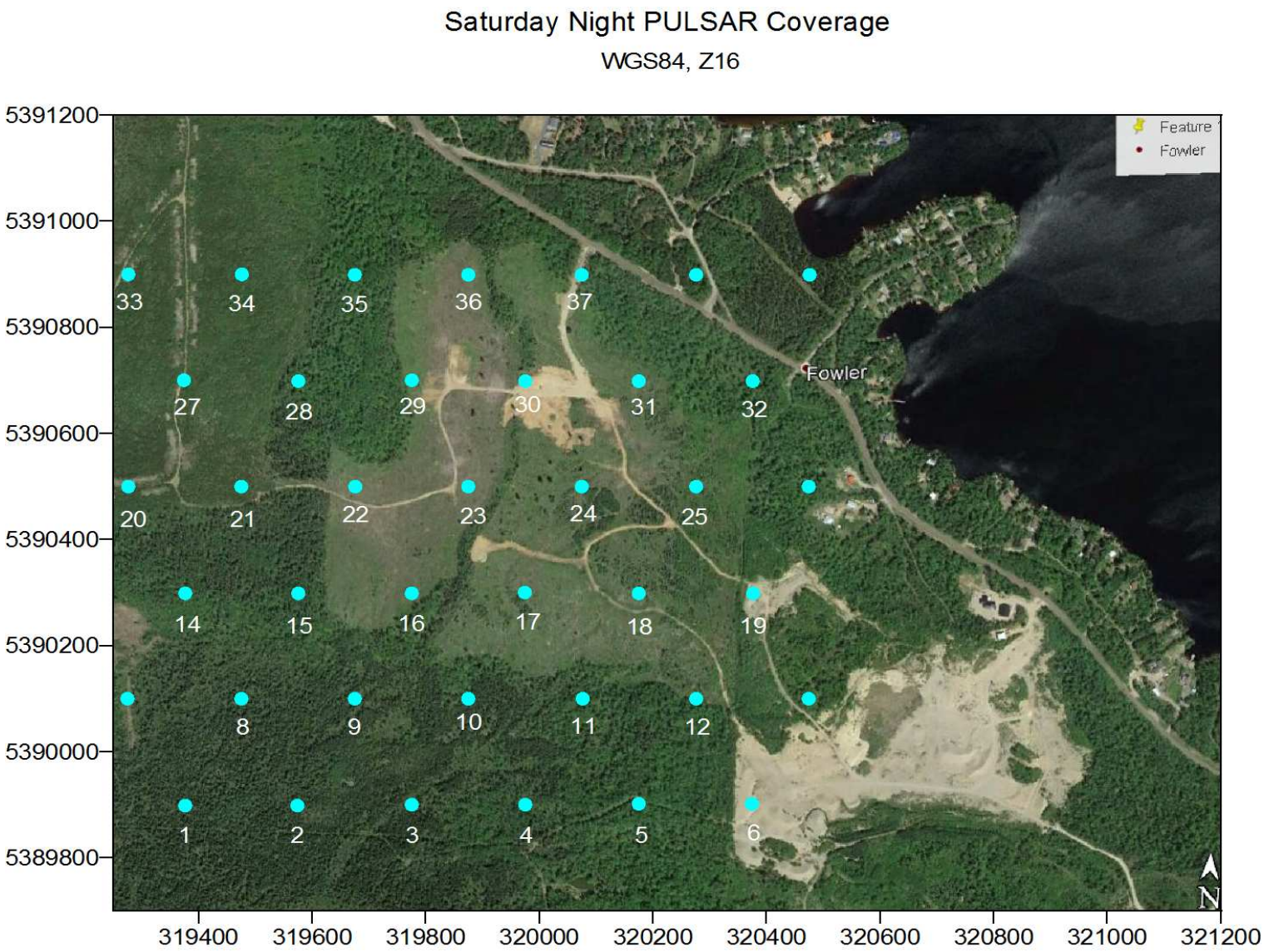

Figure 7: Satellite Imagery

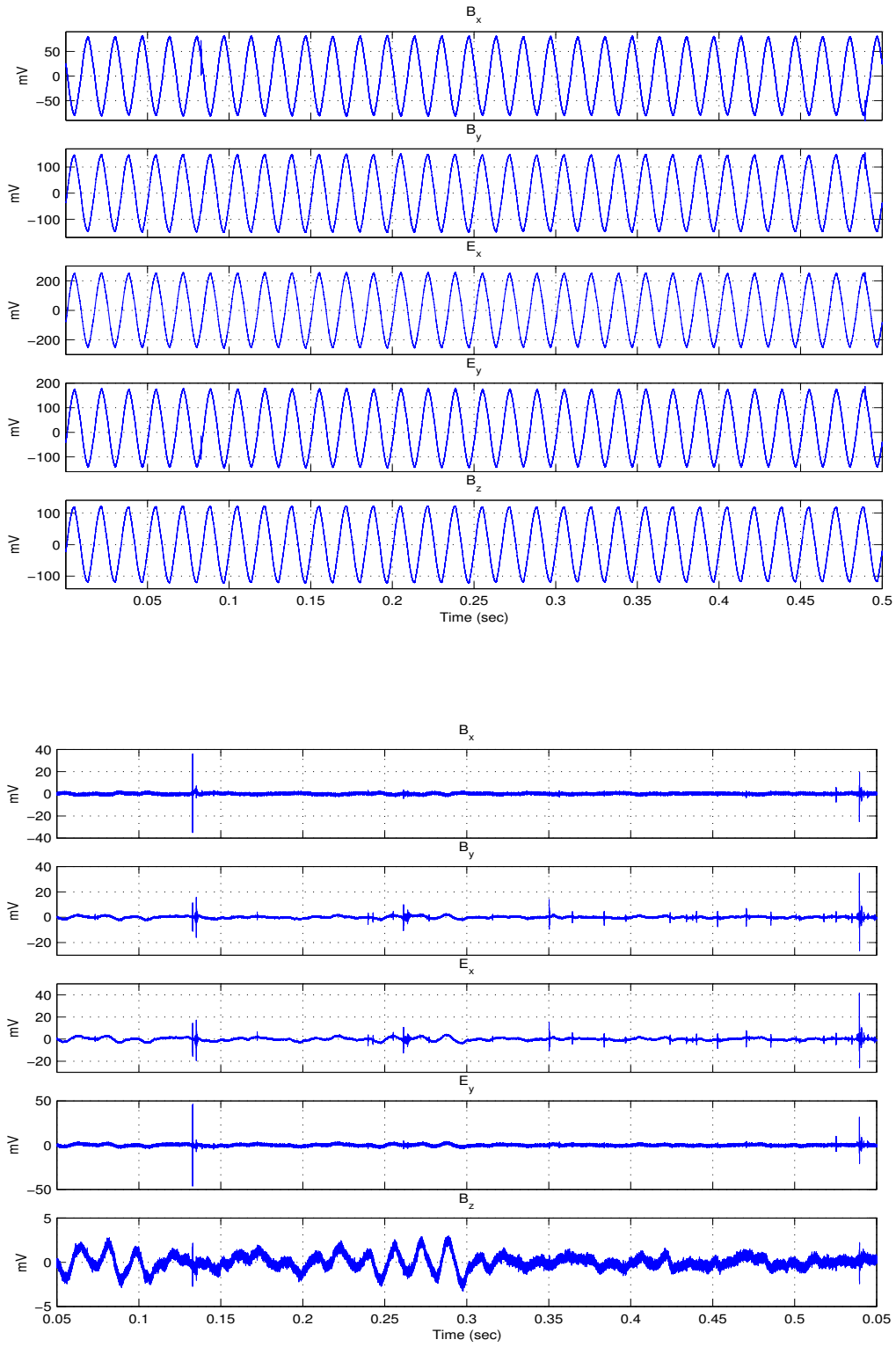

Figure 8: Powerline Noise Removal

3 Discussion

Three-dimensional inversion of the phase tensor, and joint inversion of the phase tensor/tipper/horizontal magnetic transfer functions have revealed a model which, in plan view, has the appearance of a linear resistive "finger", or perhaps a central resistive "core", with two main anomalous areas of interest; one being at the West end of the grid (L3/L4/L5), where a large vertical offset implies the presence of significant fault structure, and a deeper, more conductive anomaly at the SW edge of the grid which may represent a deep footwall depression target.

Shown in Figure 9 is the 50 to 70 m plan view which appears to map near surface gravel/sands as a N-S trending moderate resistivity low[5].

Shown in Figure 10 is the 150 to 170 m plan view where conductive material trending NE-SW is most likely due to hydrothermally altered (hematized) granite, as was encountered in DDH SN-16-001 over this depth range.

At the 360 to 390 m depth level (Figure 11), and the 540 to 580 m depth level (Figure 12) the resistive inner "core" or "finger" becomes quite prominent. Drillhole SN-16-001 intersects this feature quite well and would presumably represent the mafic intrusive encountered over this depth range, with the bottom of the intrusive being seen at $\approx$ 520 m depth (Transition Metals press release, January 23, 2017).

The vertical offset that occurs along the western edge of the resistive "finger" is best seen in vertical cross section down L3 (Figure 19). Note the difference in elevation of resistive (red) material at station 16MS as compared to 15MS/14MS. The vertical offset occurs approximately 300 m West of DDH SN-16-001 and would presumably be an area of interest for further drilling. This is also seen on L4 (Figure 20) where again we note the difference in elevation of resisitve (red) material between stations 22MS and 21MS. The vertical offset also coincides with the location of a change in orientation of the resistive "finger" seen on the plan view phase tensor inversion plots.

The vertical cross section plots, especially the phase tensor alone, appear to show the base of the intrusion as a bowl like surface, which is to be expected (pers. comm. Mr. Grant Mourre). Moreover, the "bowl" is very broad on L1 (Figure 17) and L2 (Figure 18), essentially spanning the entire line length, and extending to great depth, $\approx$ 1200 m, but on L3/L4, the "bowl" becomes compressed into a narrower "channel" with a relatively flat portion on the East end of L3/L4 and a sudden vertical drop into the "channel" in the vicinity of stations 15MS/22MS.

The transition from "bowl" to "channel" like may be due to fault structure which occurs in the same orientation as the resistive "finger". This is consistent with a fault indicated on a Transition Metals press release dated January 23, 2017 (see Figure 1 in press release), and also with a clear break in the total field magnetics data in the same orientation (Figure 23).

At approximately 1000 m depth, near the SW edge of the grid, a strong resistivity low is seen which is common to all the inverted models (Figure 14, 15, 17 and 18). Although more coverage to the South would be desirable to better image this anomaly, this strong resistivity low may represent a footwall depression target, where PGM mineralization is expected to accumulate (pers. comm. Mr. Grant Mourre).

[5]Left hand panels indicate phase tensor alone while right hand panels joint phase tensor/tipper/horizontal magnetic transfer function.

The anomalous areas identified in the PULSAR survey generally occur on the gradient of the potential field data (Figure 23).

As can be seen in Figures 24 to 41, the 3D inversion code was able to fit the Saturday Night data quite well, the base station location chosen for horizontal magnetic transfer function estimation seems to have been a reasonable one. Near field effects due to source field interaction with the nearby powerline was much less severe as compared to Aer-Kidd, as a result, the tipper data was well used, and well fit, to sub 10 Hz.

It is interesting to note that one can clearly see the character change in the measured data between the three southern-most lines (1MS to 19MS) as compared to the three northern-most lines (20MS to 37MS), especially so with the tipper data (Figures 26, 27), indicative of the structural change in the intrusive body. North of L5, we appear to lose the intrusive body, however, more coverage to NE would be desirable to confirm this more clearly.

Although the horizontal MTF's were well fit by the 3D inversion code, it's not known how well the chosen base station location truly approximated background geology. Until such time as a permament base station is established outside of Dalmeny, in a 1D earth, this question will not be completely answered. In the meantime, it may be beneficial to re-do the MTF inversion by using MTF's transformed to use one of the measurement stations as the base station. We are also working on a newer version of our inversion code which will account for the resistivity structure under the MTF base station, thus modeling and taking into account any local anomaly distortion effects.

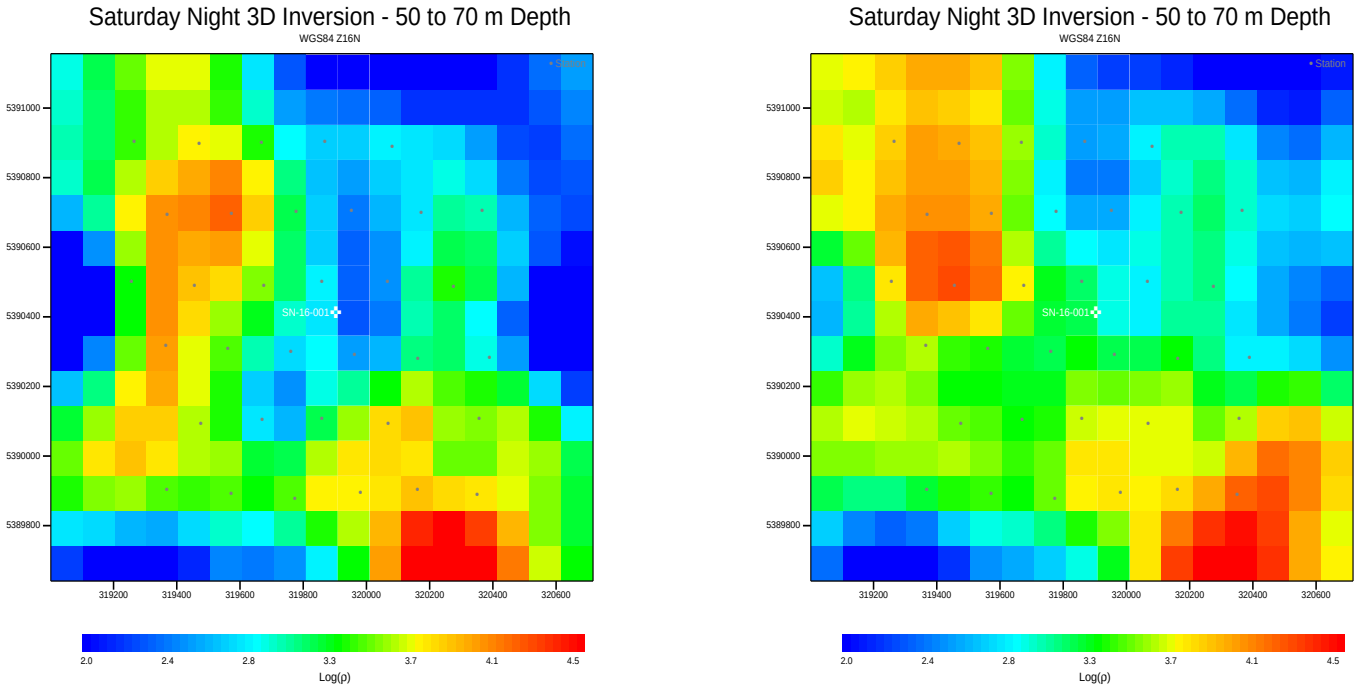

Figure 9: 50 to 70 m Plan View

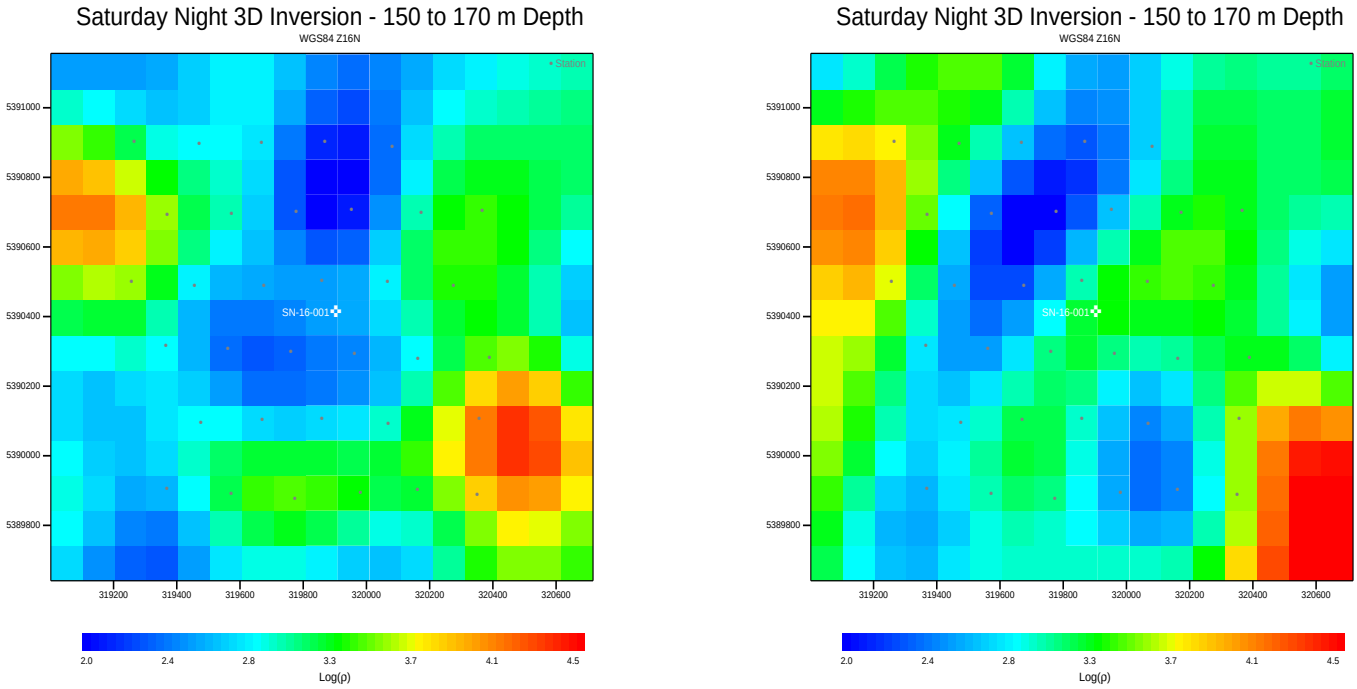

Figure 10: 150 to 170 m Plan View

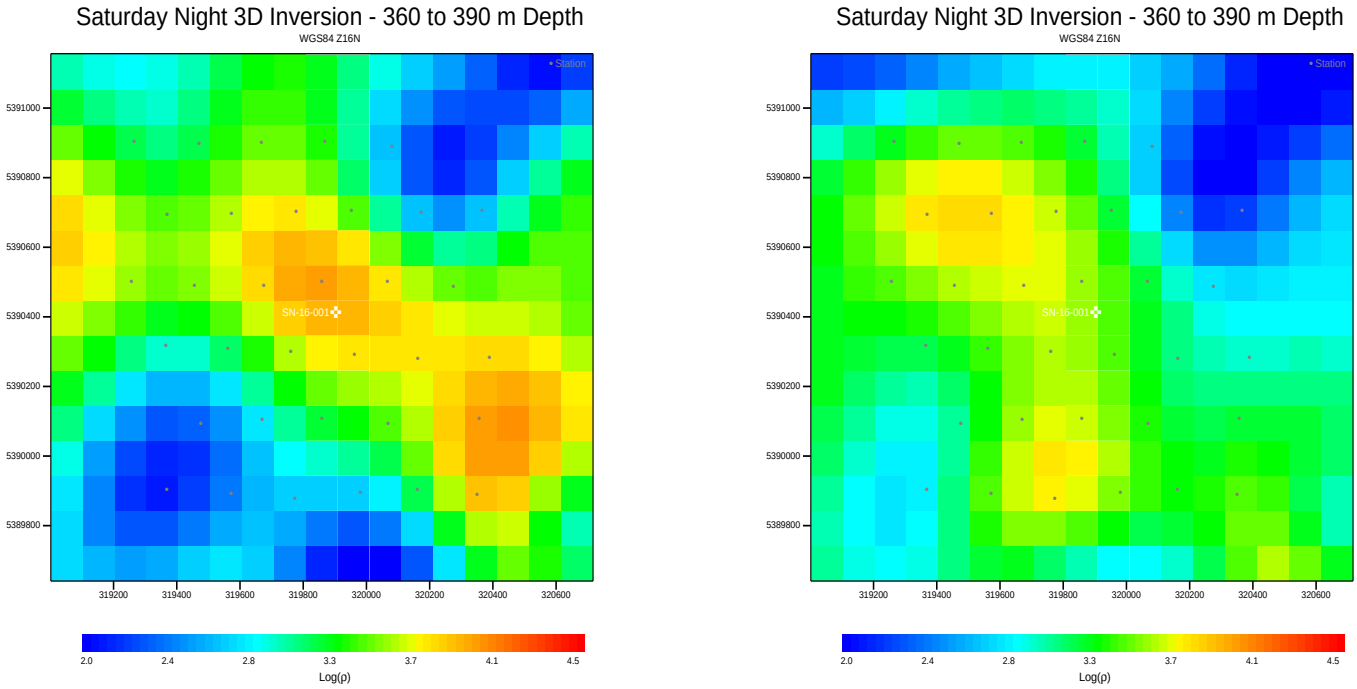

Figure 11: 360 to 390 m Plan View

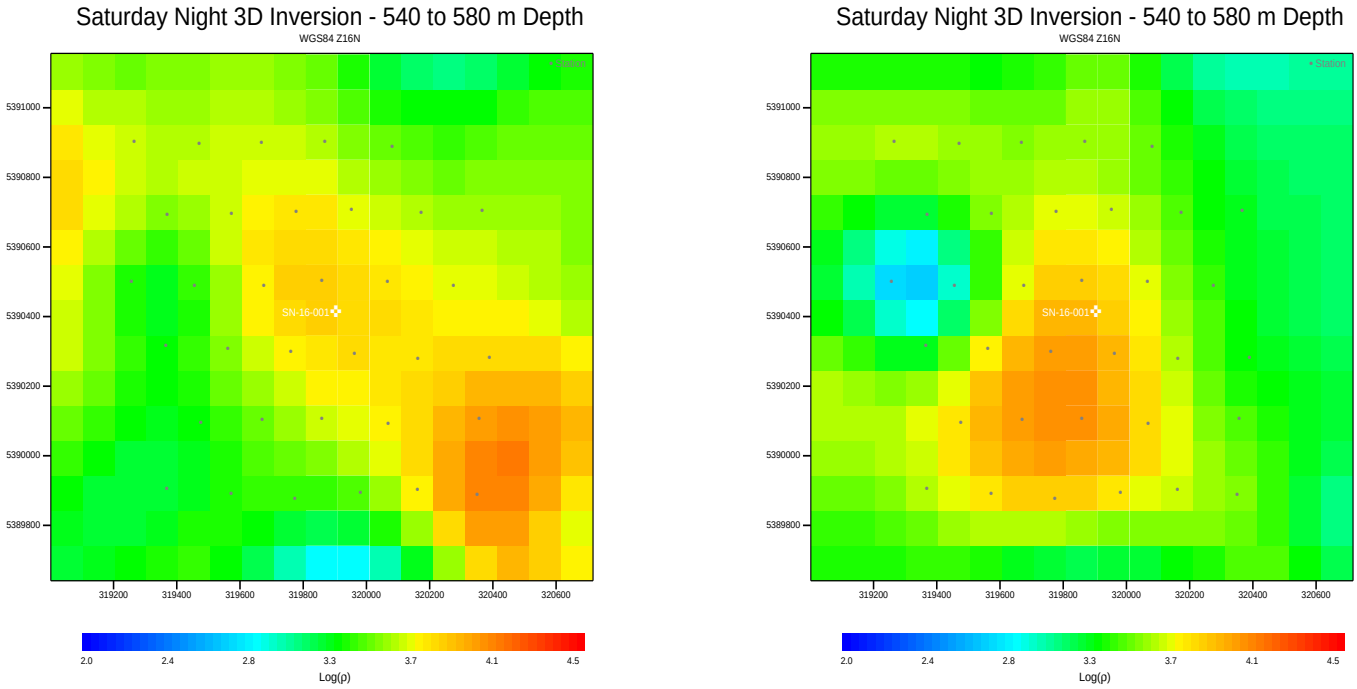

Figure 12: 540 to 580 m Plan View

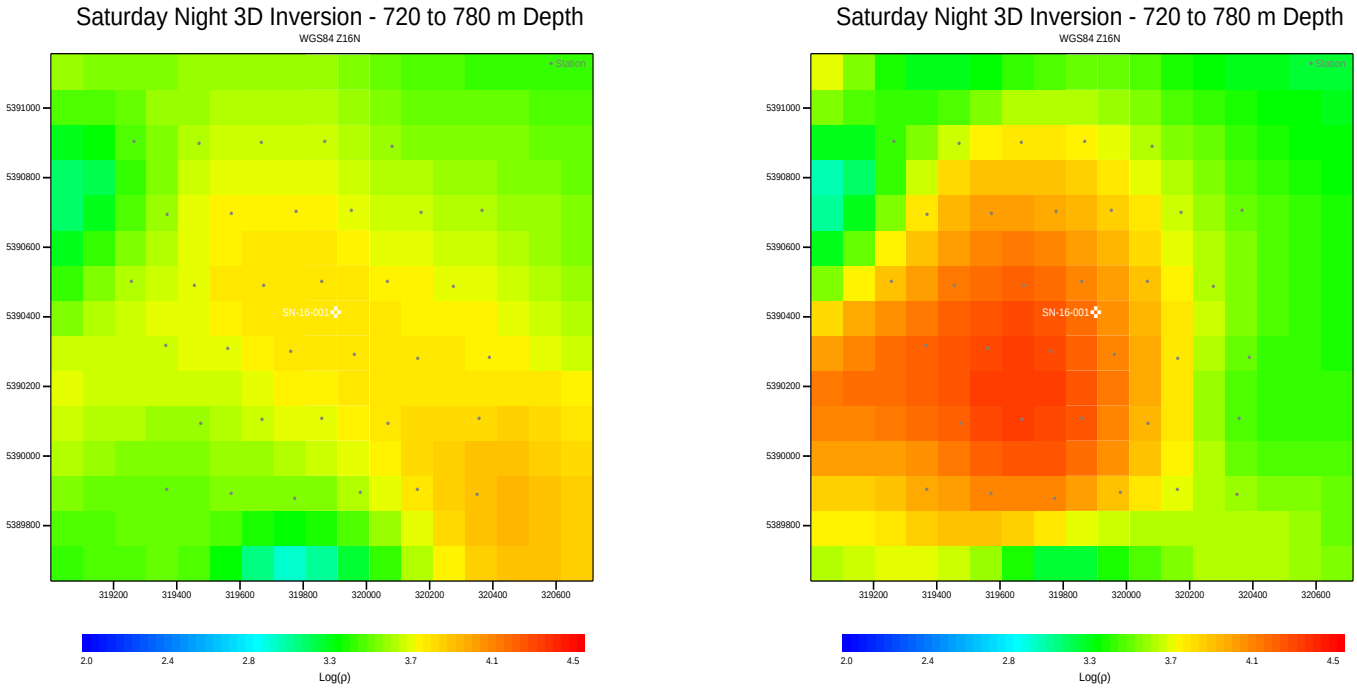

Figure 13: 720 to 780 m Plan View

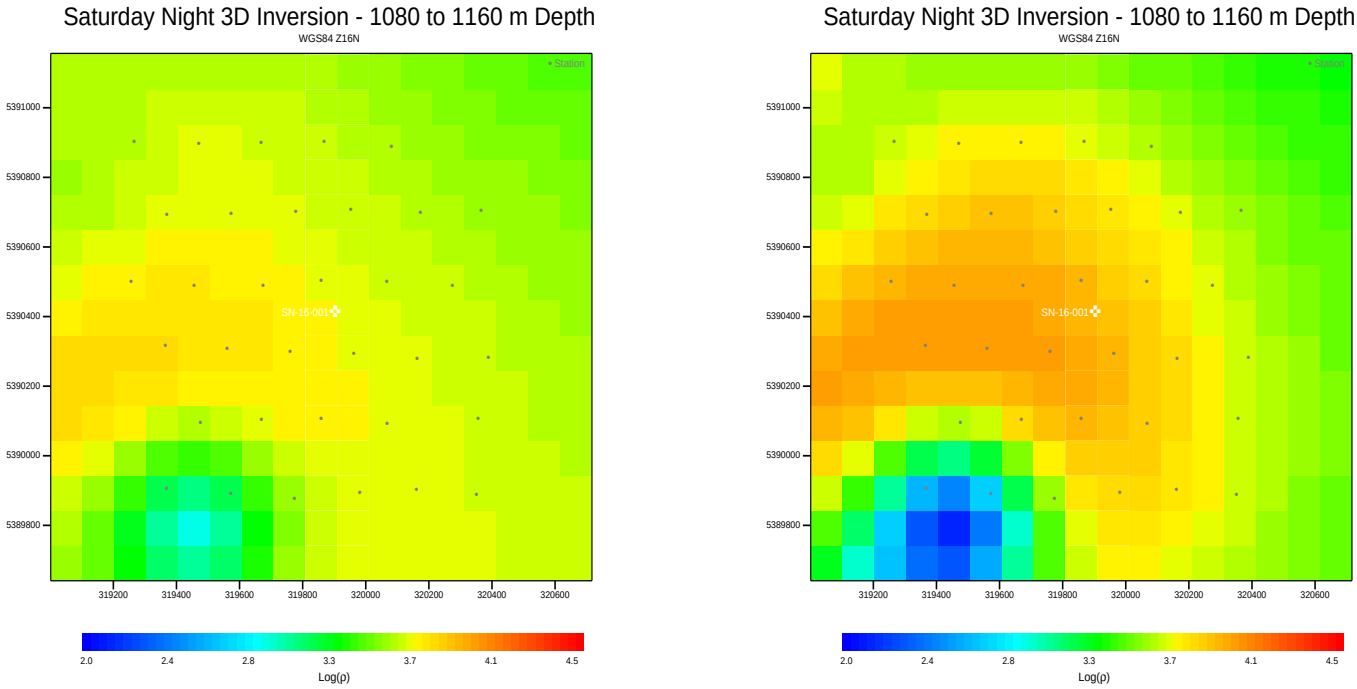

Figure 14: 1080 to 1160 m Plan View

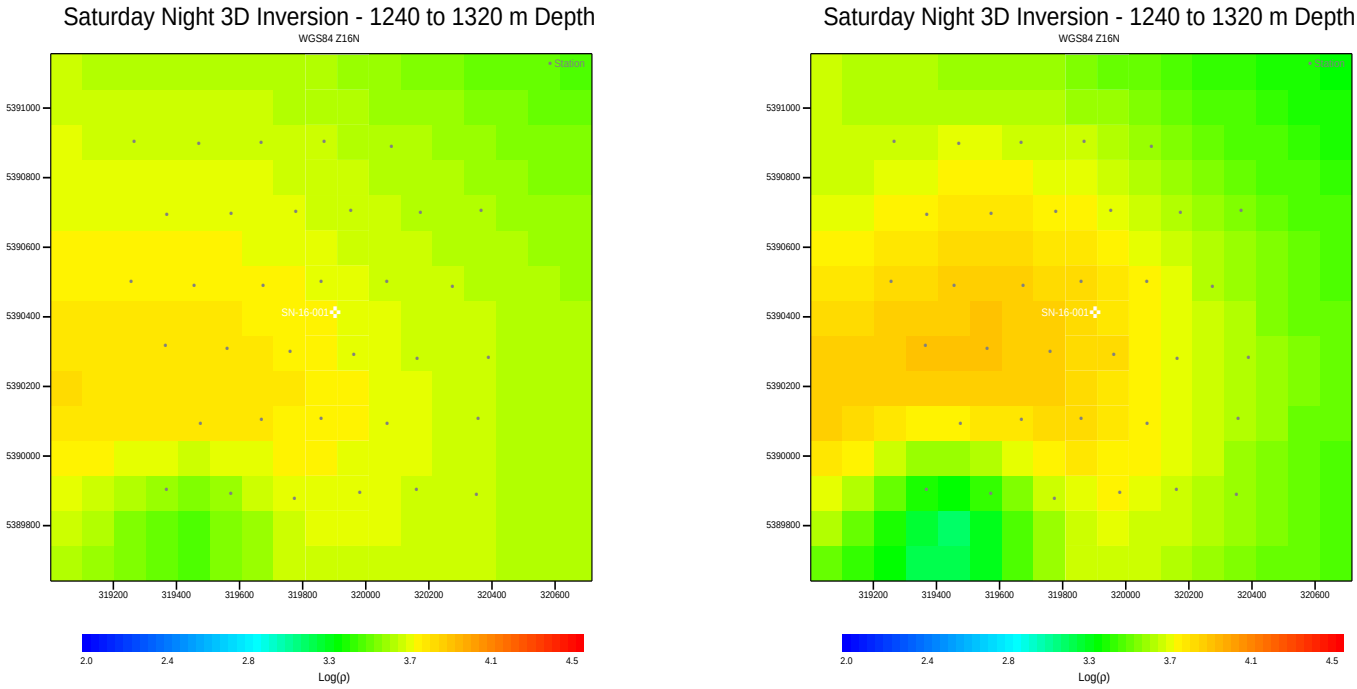

Figure 15: 1240 to 1320 m Plan View

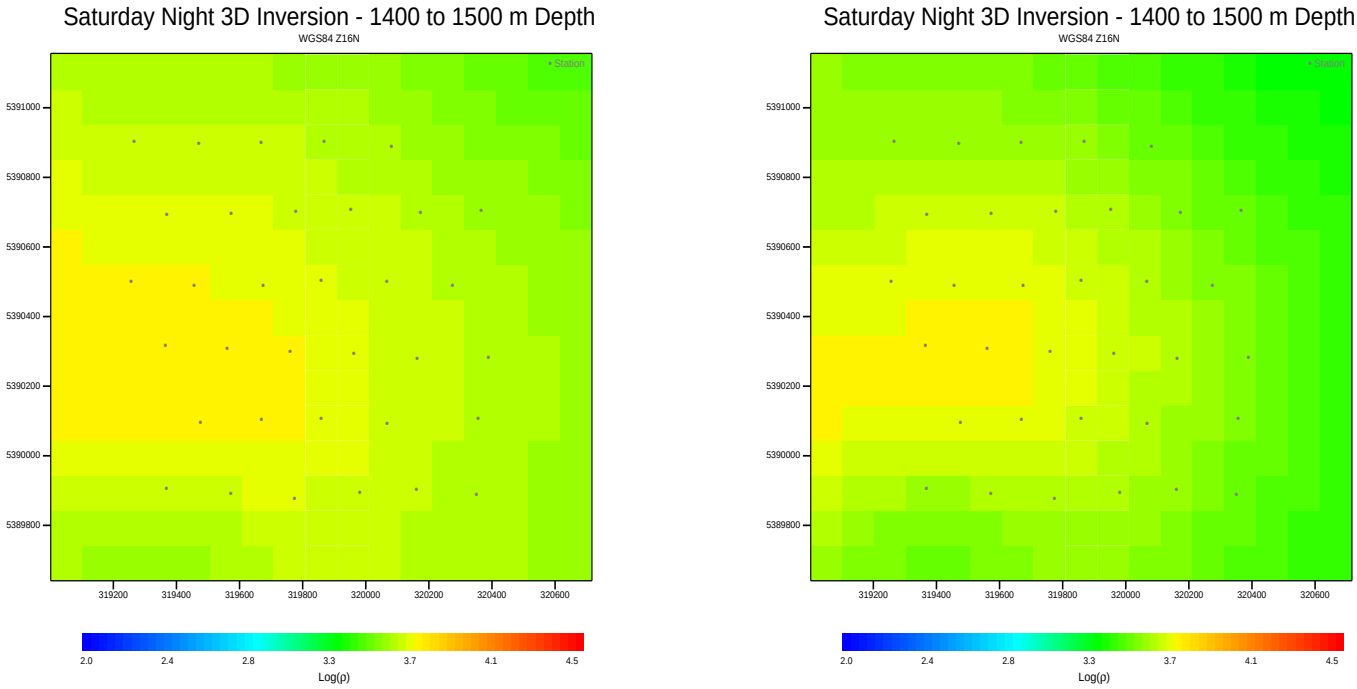

Figure 16: 1400 to 1500 m Plan View

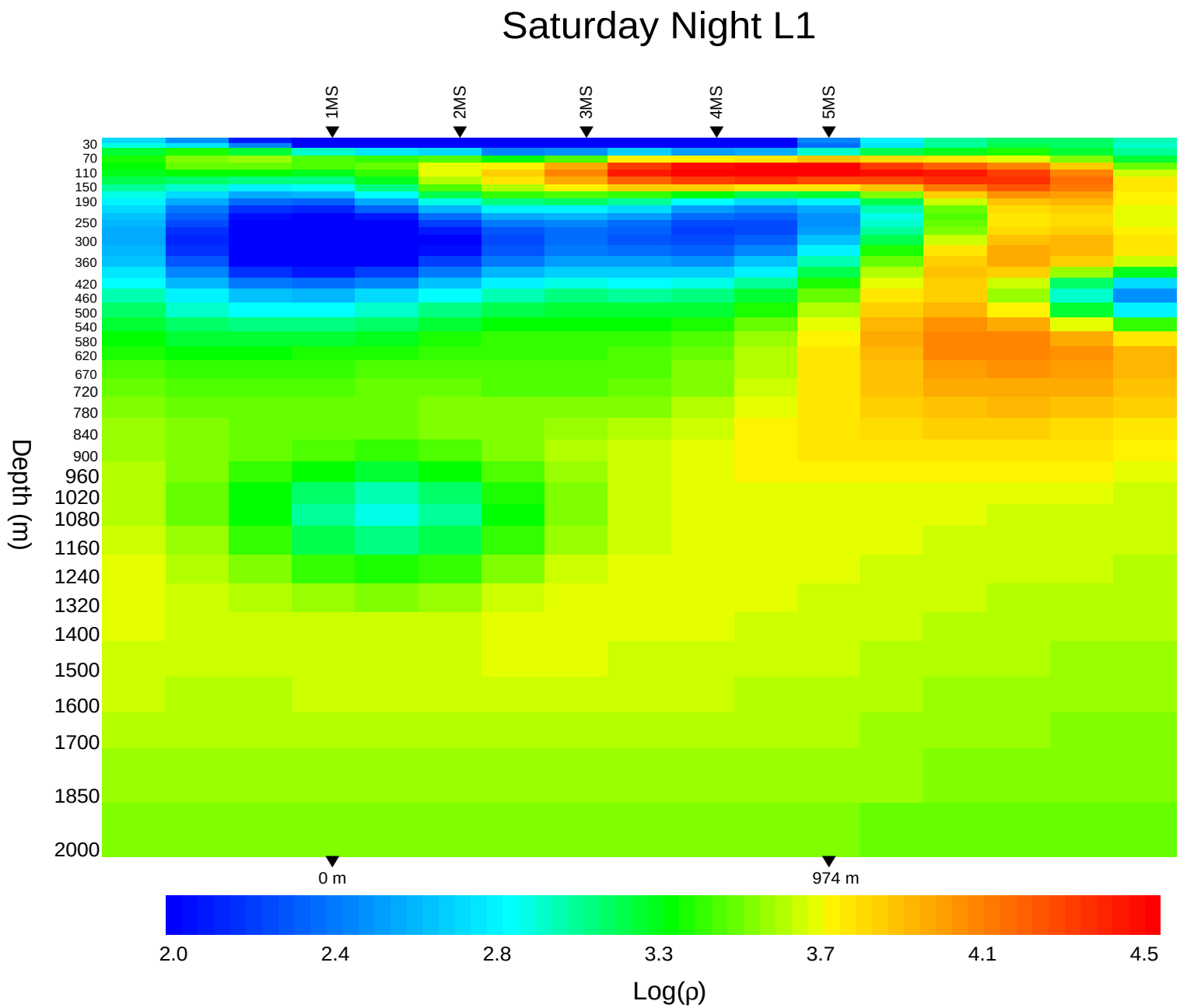

Figure 17: Phase Tensor Inversion - Vertical Slice down L1

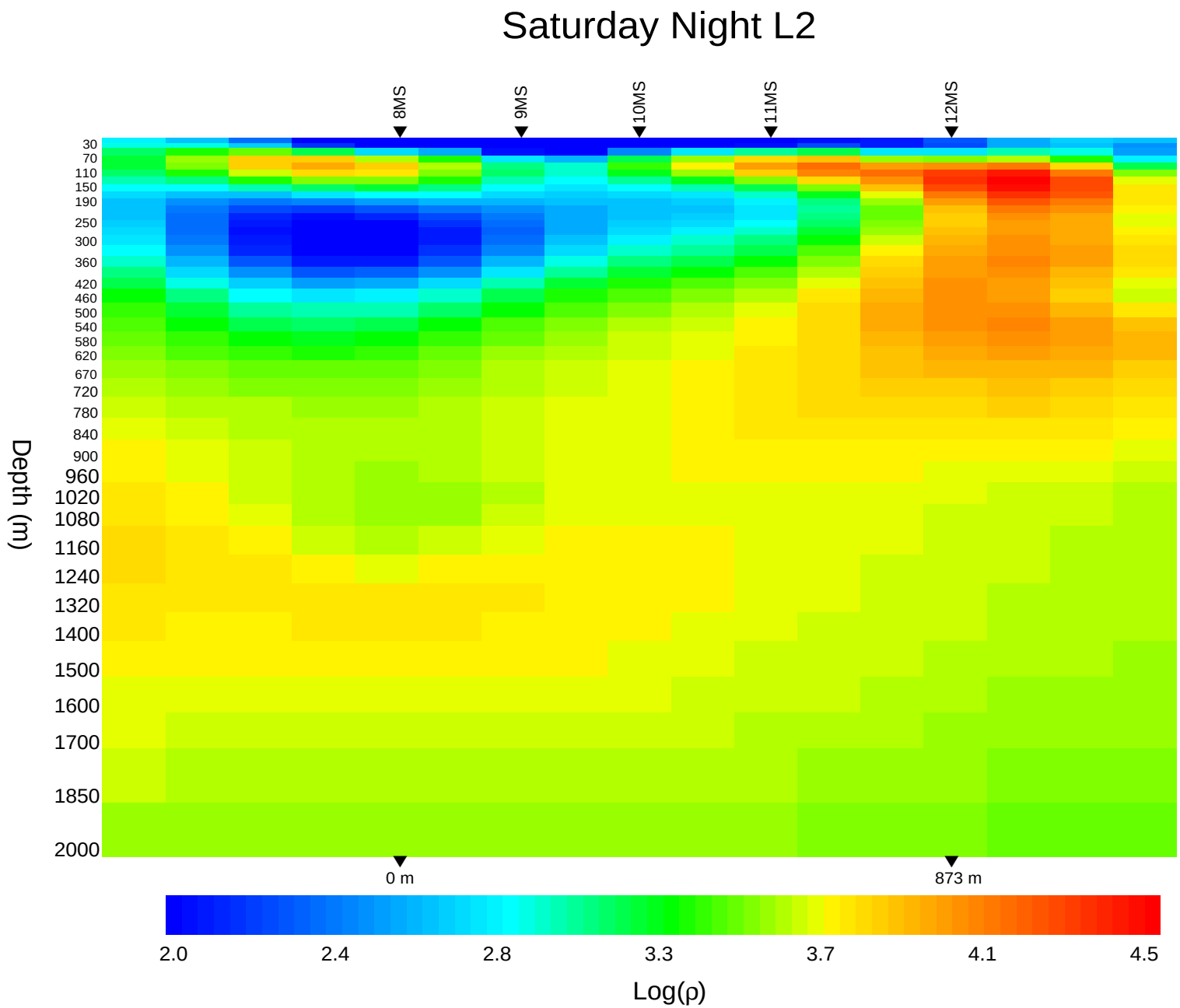

Figure 18: Phase Tensor Inversion Vertical Slice down L2

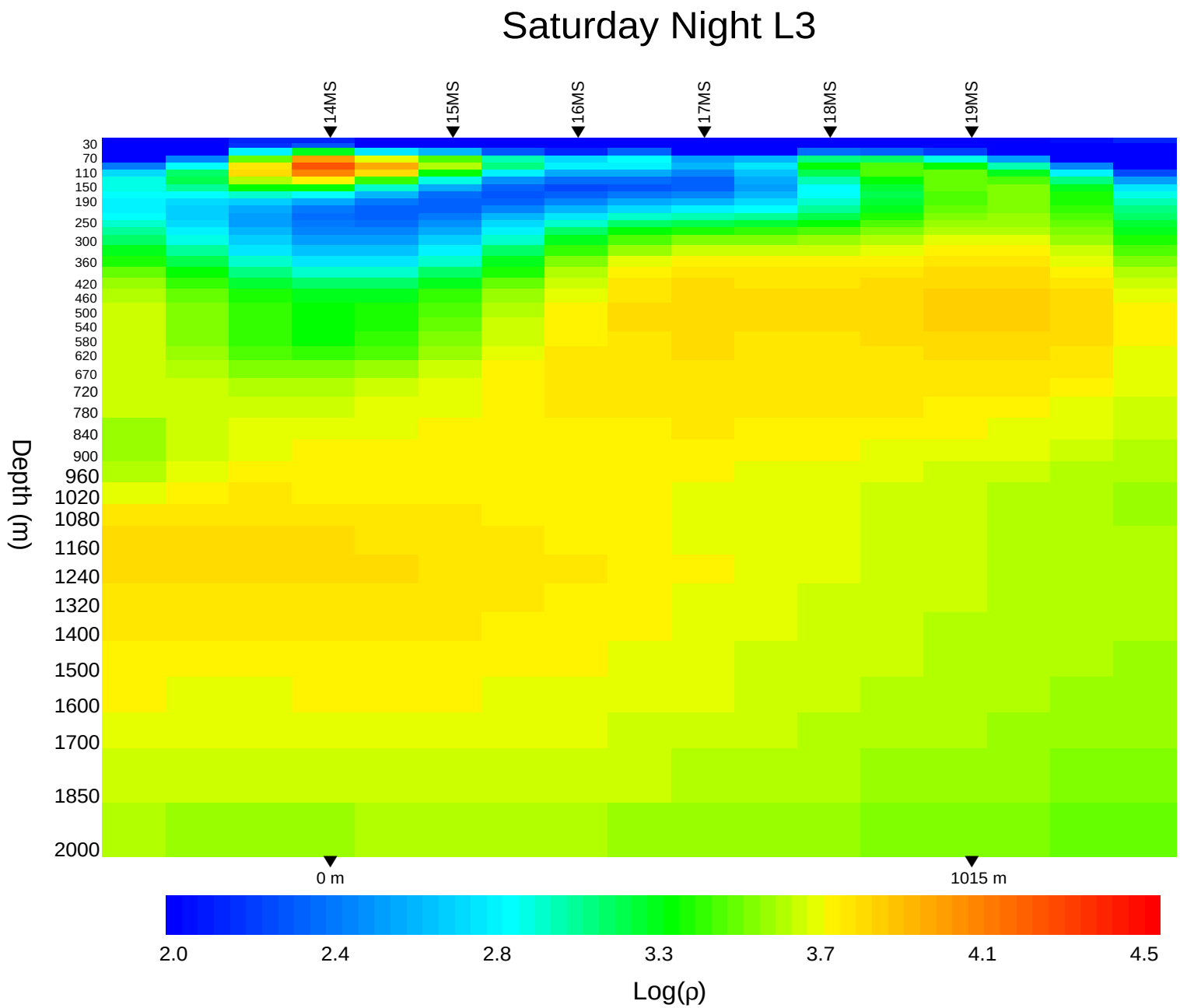

Figure 19: Phase Tensor Inversion - Vertical Slice down L3

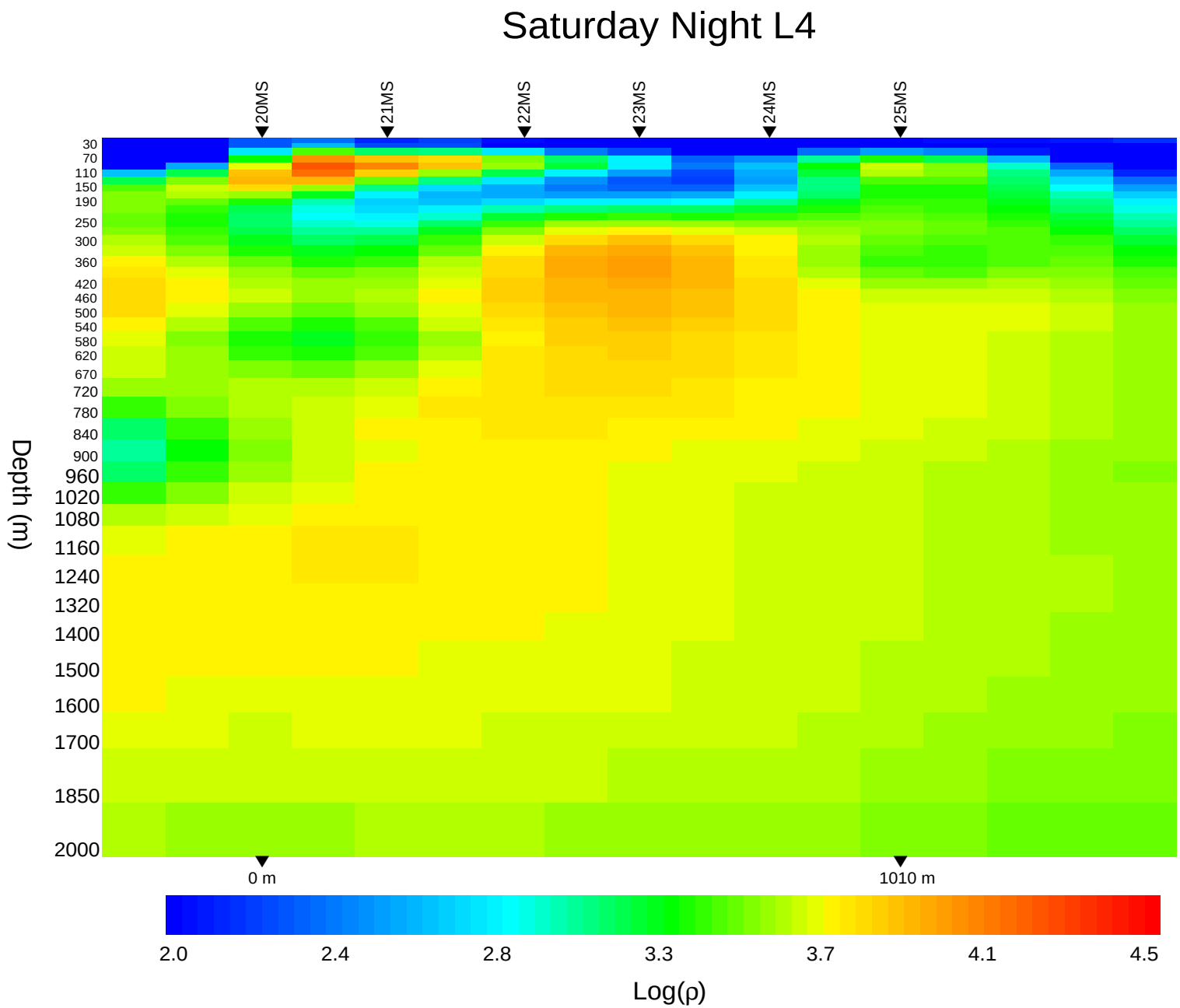

Figure 20: Phase Tensor Inversion - Vertical Slice down L4

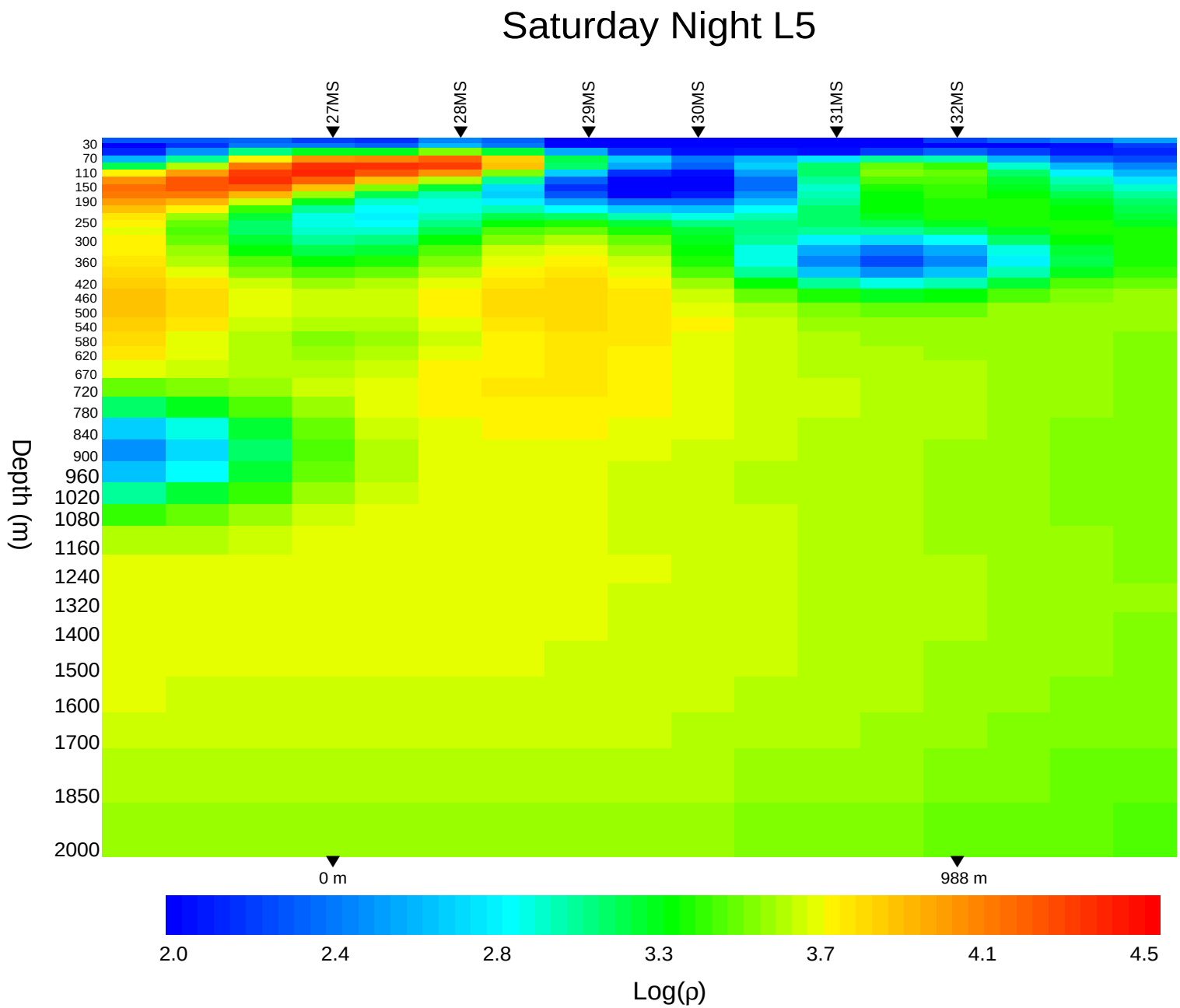

Figure 21: Phase Tensor Inversion - Vertical Slice down L5

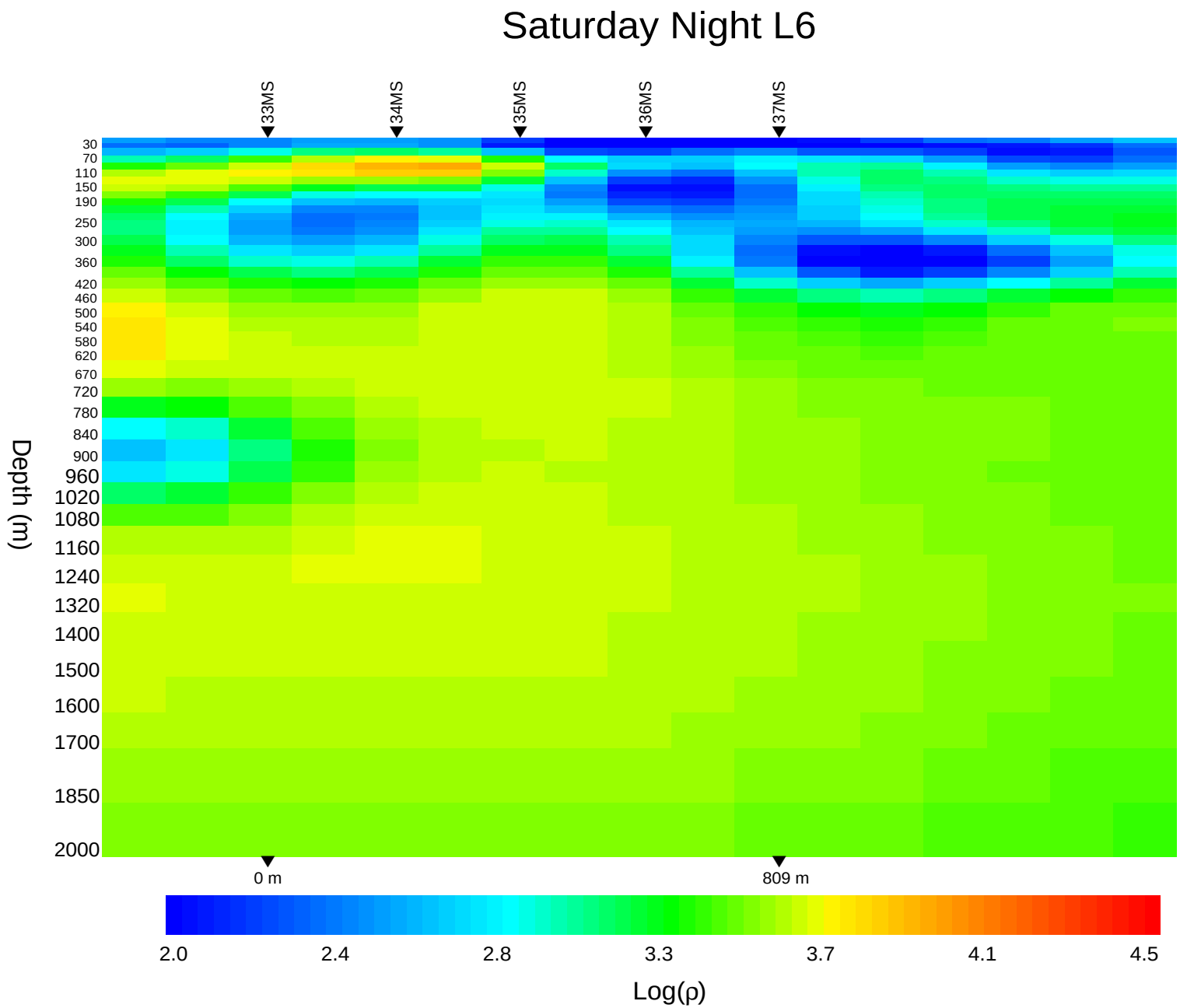

Figure 22: Phase Tensor Inversion - Vertical Slice down L6

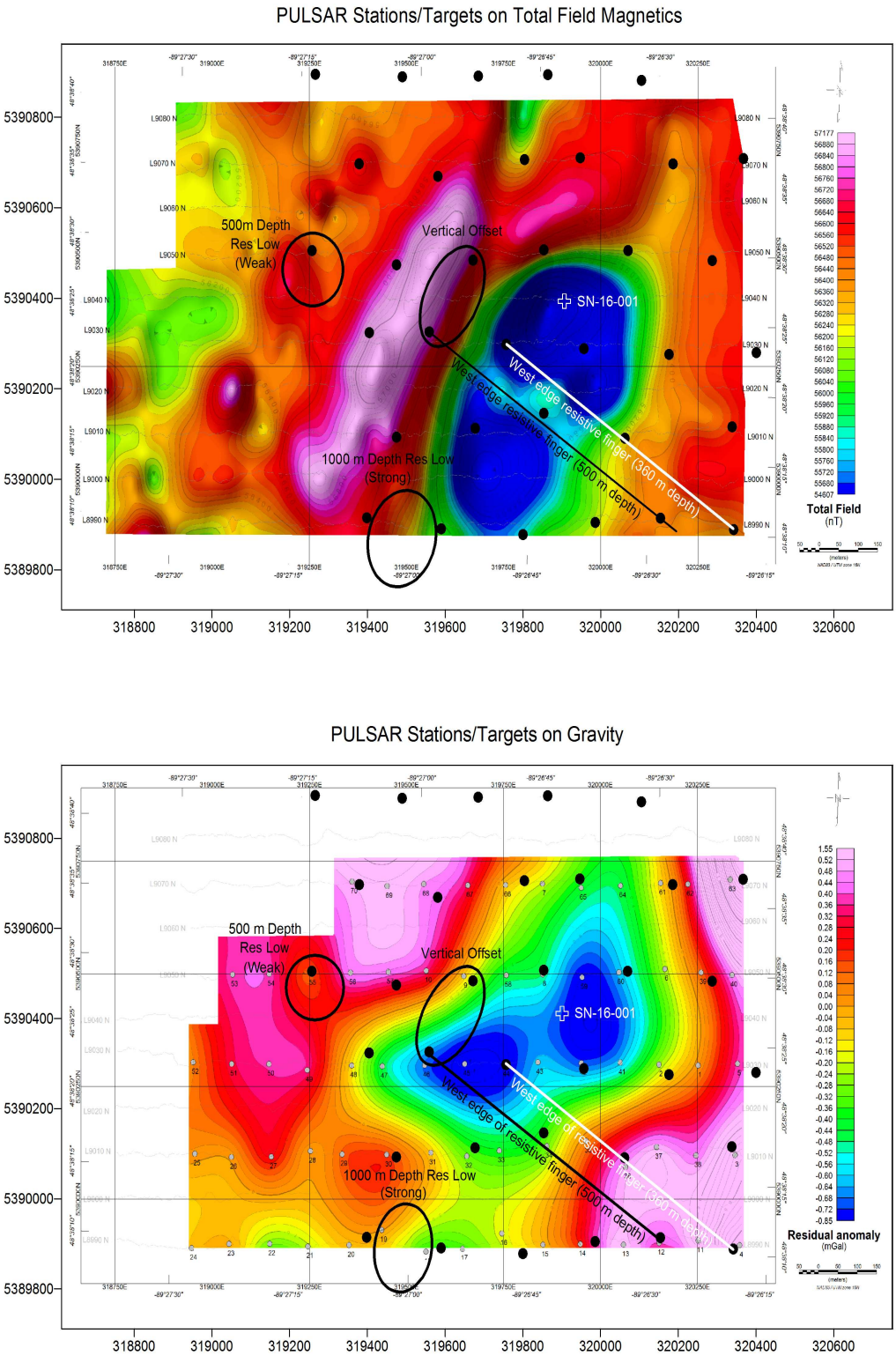

Figure 23: Potential Field Datal

References

[1] Berdichevsky, M.N., 1968, Electrical Prospecting by the method of magneto-variational profiling, Nedra, Moscow (in Russian).

[2] Berdichevsky, M.N., Kuznetsov, V.A. and Pal'shin, N.A., 2009, Analysis of Magneto-variational Response Functions, Physics of the Solid Earth, **45**, no. 3, 179-198.

[3] Caldwell, T.G., Bibby, H.M. and Brown, C., 2004, The magnetotelluric phase tensor, Geophysical Journal International, **158**, 457-469.

[4] Campanya, J., Ogaya, X., Jones, A.G., Rath, V., Vozar, J. and Meqbel, N., 2016, The advantages of complementing MT profiles in 3-D environments with geomagnetic transfer functions and inter-station horizontal magnetic transfer function data: Results from a synthetic case study, Geophysical Journal International.

[5] deGroot-Hedlin, C. and Constable, S., 1990, Occam's inversion to generate smooth, two-dimensional models from magnetotelluric data, Geophysics,**55**, 1613-1624.

[6] Gamble, T.D., Goubau, W.M. and Clarke, J., 1979, Error analysis for remote reference magnetotellurics, Geophysics, **44**, 959-968.

[7] Goldak, D.K. and Goldak, M.S., 2001, Transient Magnetotellurics with Adaptive Polarization Stacking, SEG International Exposition and 71'st Annual Meeting, San Antonio, 1509-1512.

[8] Jones, D.L. and Kemp, D.T., 1971, The nature and average magnitude of the sources of transient excitation of Schumann resonances, Journal of Atmospheric and Terrestrial Physics, **33**, 557-566.

[9] Mueller, C., Bellefleur, G., Adam, E., Perron, G., Mah, M. and Snyder, D., 2012, Performance of low-fold scalar migration for downhole seismic imaging of massive sulfide ore deposits at Norman West, Sudbury, Canada, Geophysics, **77**, WC3-WC13.

[10] Pierce, E.T., 1977, Atmospherics and radio noise, in Golde, R.H., ed., Lightning, **1**, Academic Press.

[11] Snyder, D.G., Perron, G., Pflug, K. and Stevens, K., 2002, New insights into the structure of the Sudbury Igneous Complex from downhole seismic studies, Canadian Journal of Earth Sciences, **39**, 943-951.

[12] Siripunvaraporn, W., Egbert, G., Lenbury, Y. and Uyeshima M., 2005, Three-dimensional magnetotelluric inversion: data-space method, Physics of the Earth and Planetary Interiors, **150**, 3-14.

[13] Tietze, K., Ritter, O. and Egbert, G.D., 2015, 3-D joint inversion of the magnetotelluric phase tensor and vertical magnetic transfer functions, Geophysical Journal International, **203**, 1128-1148.

[14] Volland, H., 1982, Low frequency radio noise: in Volland, H., ed., CRC Handbook of Atmospherics, **1**, CRC Press Inc.

4 Appendix

4.1 Measured Data

Figure 24: Measured Phase Tensor Φ_{xx}, Φ_{xy}

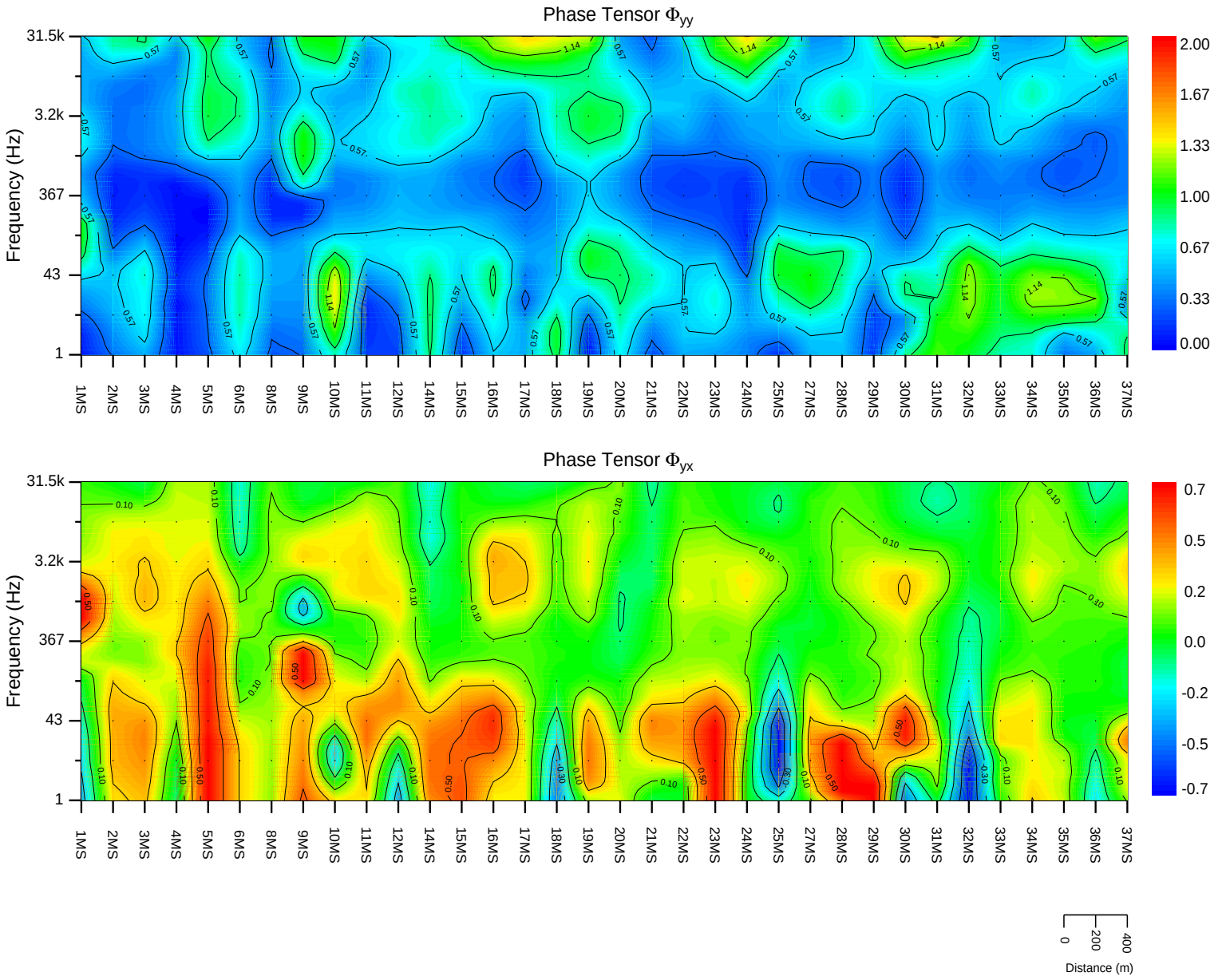

Figure 25: Measured Phase Tensor Φ_{yx}, Φ_{yy}

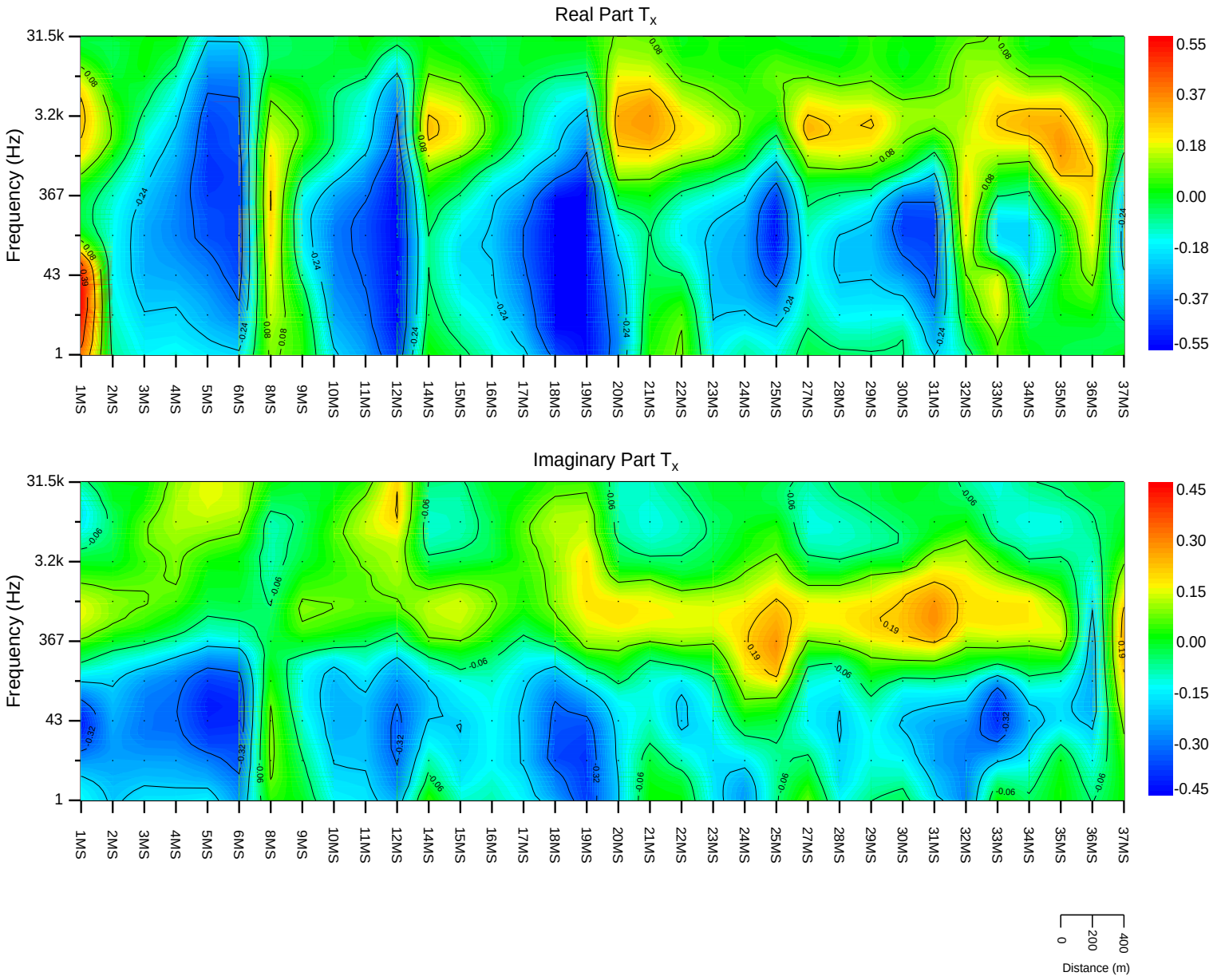

Figure 26: Measured T_x

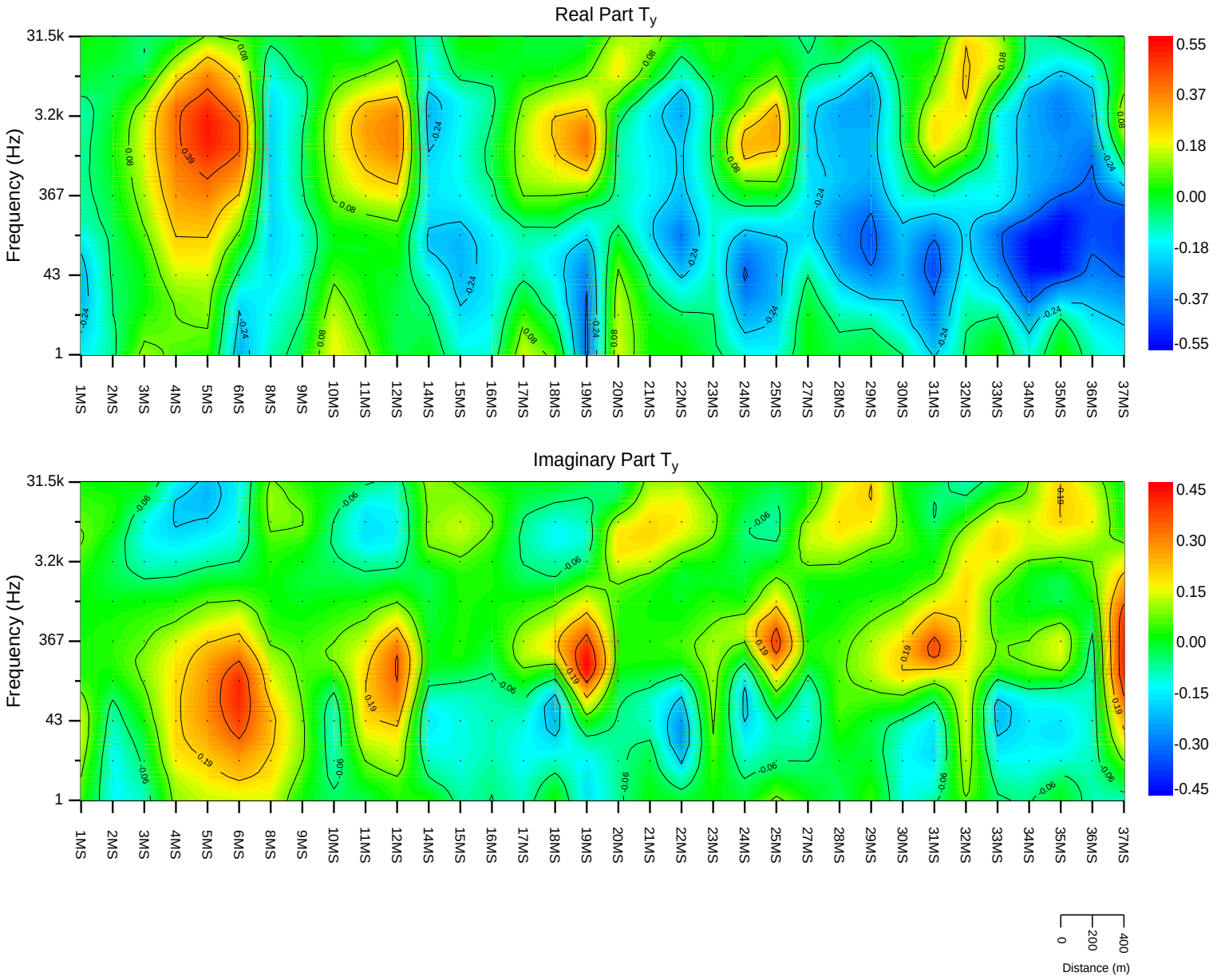

Figure 27: Measured T_y

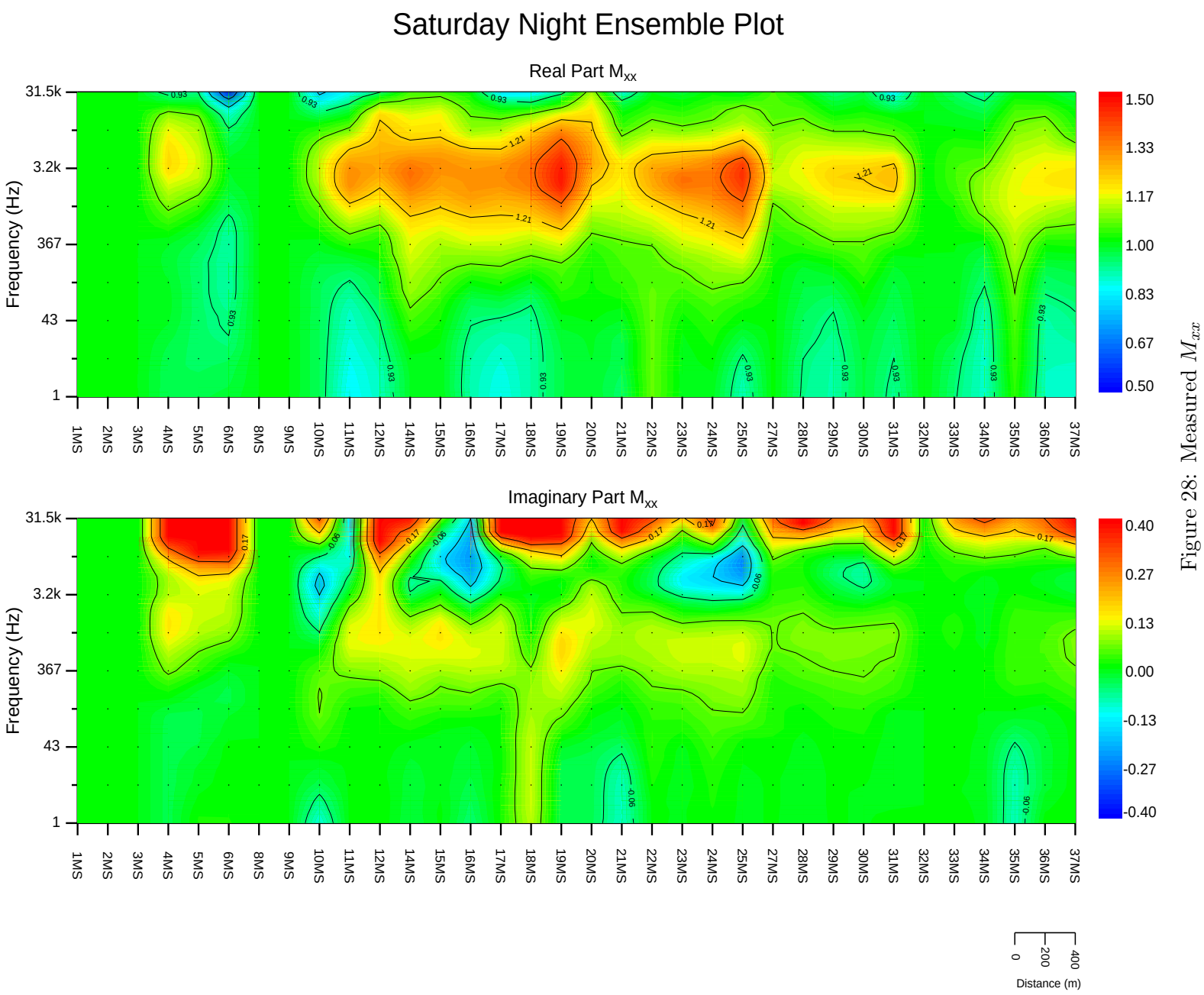

Figure 28: Measured M_{xx}

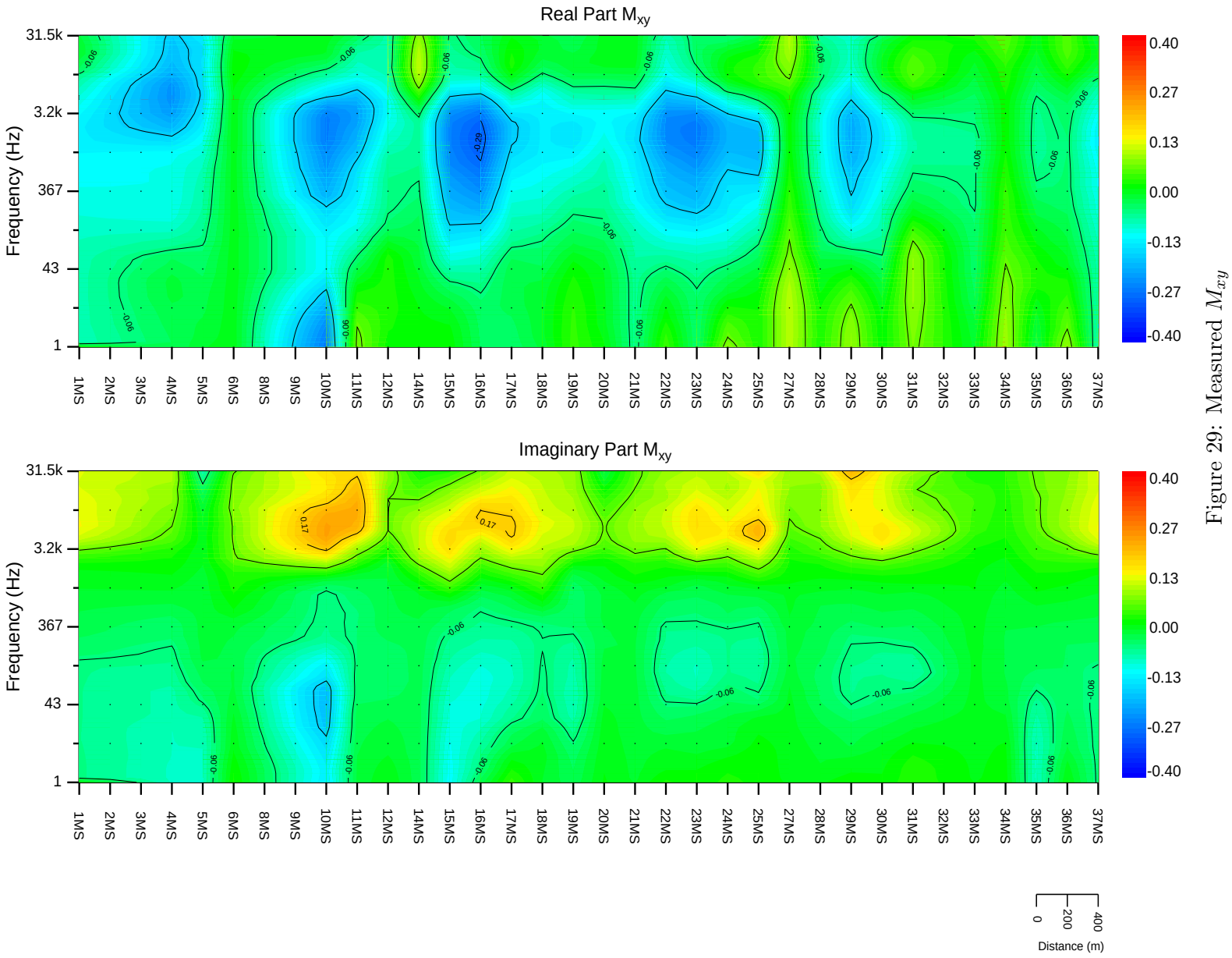

Figure 29: Measured M_{xy}

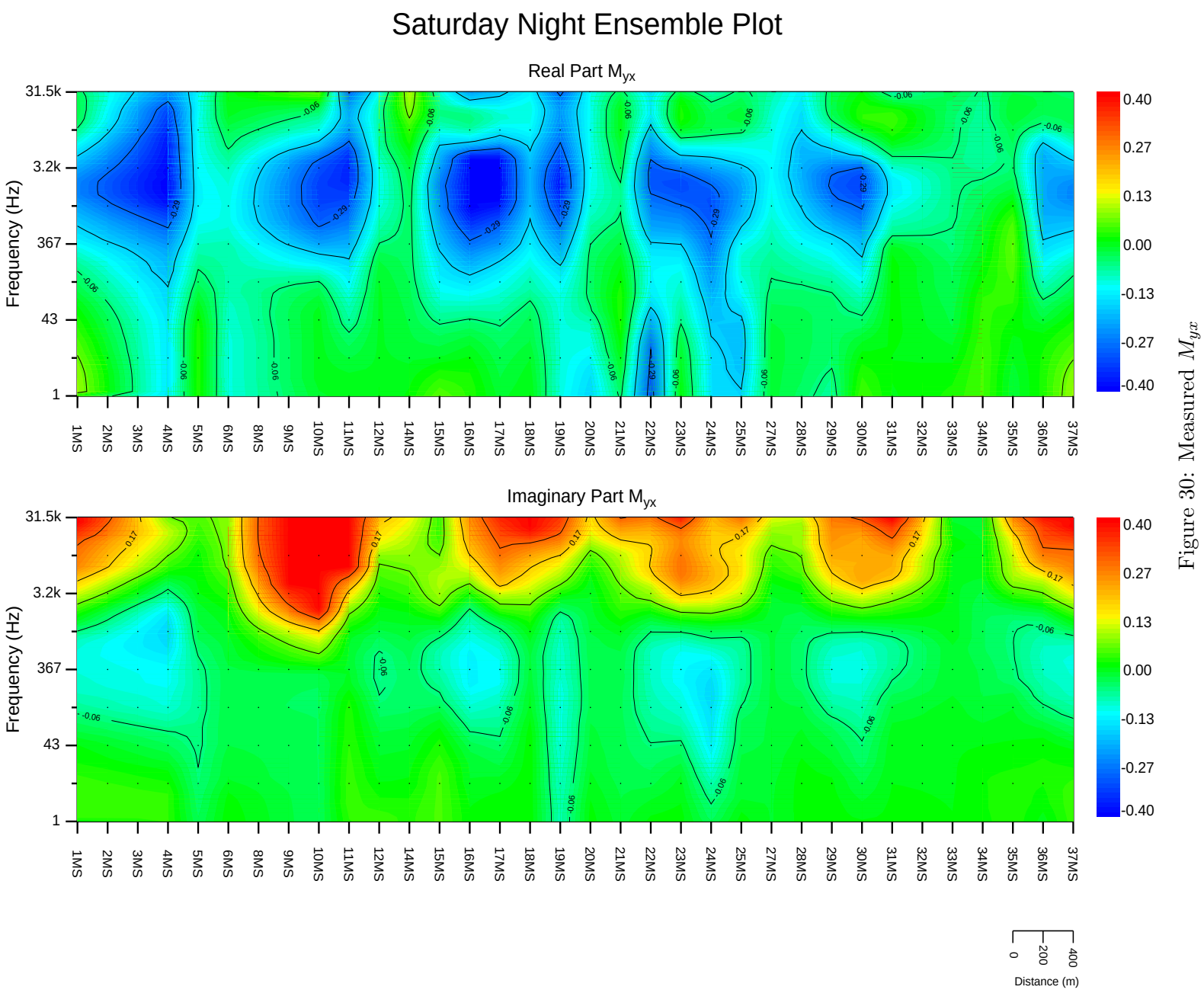

Figure 30: Measured M_{yx}

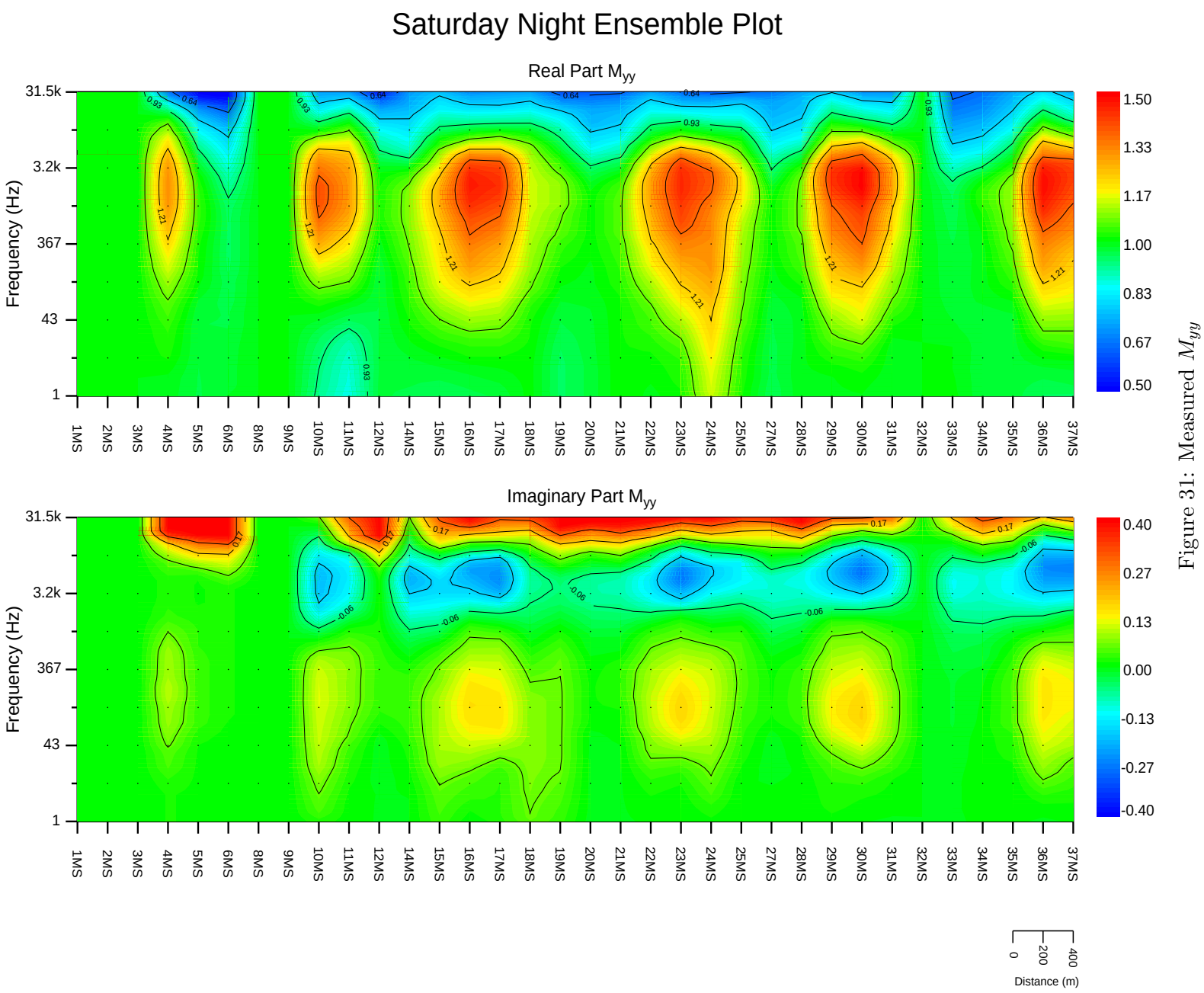

Figure 31: Measured M_{yy}

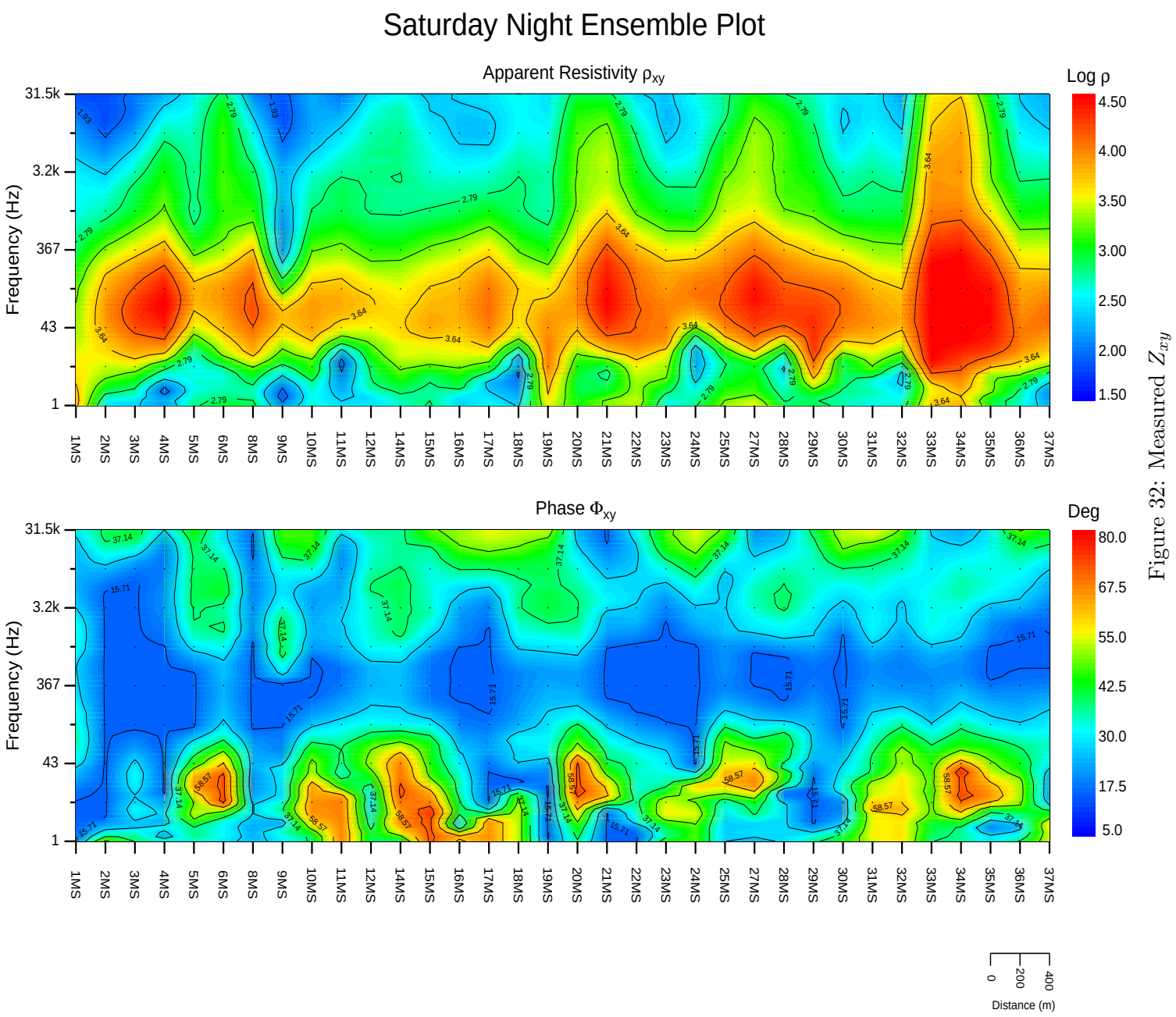

Figure 32: Measured Z_{xy}

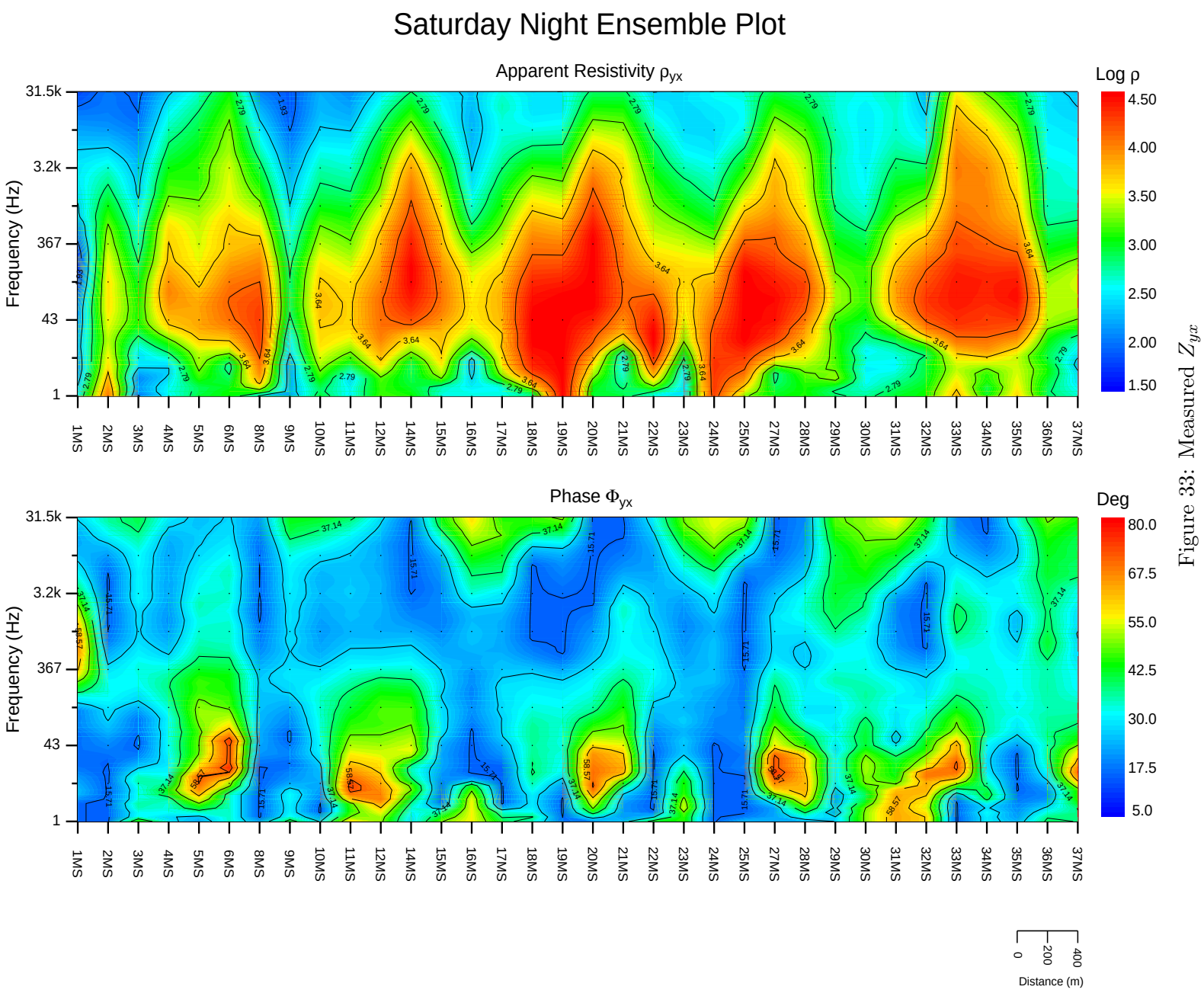

Figure 33: Measured Z_{yx}

4.2 Modeled Data

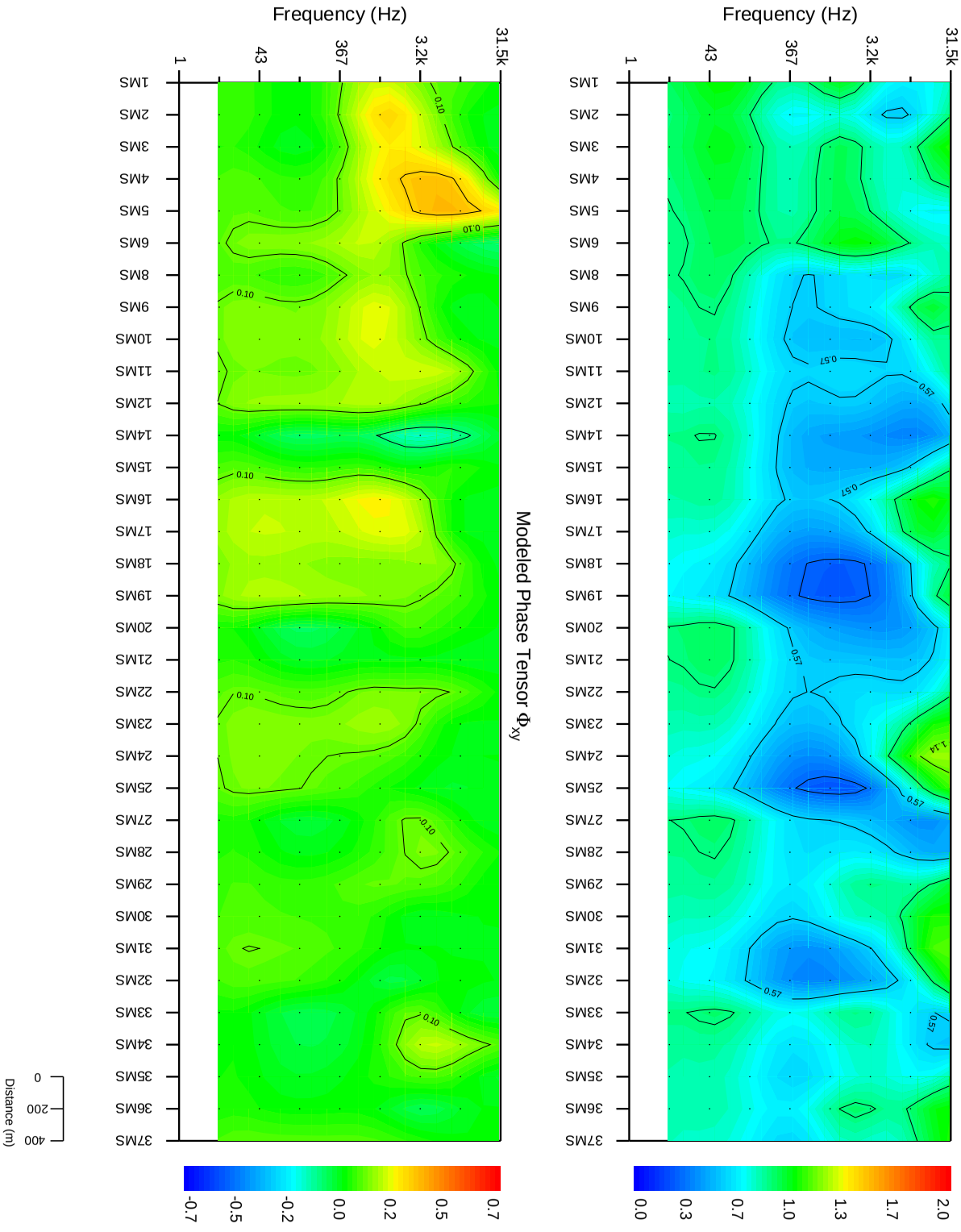

Figure 34: Modeled Phase Tensor Φ_{xx}, Φ_{xy}

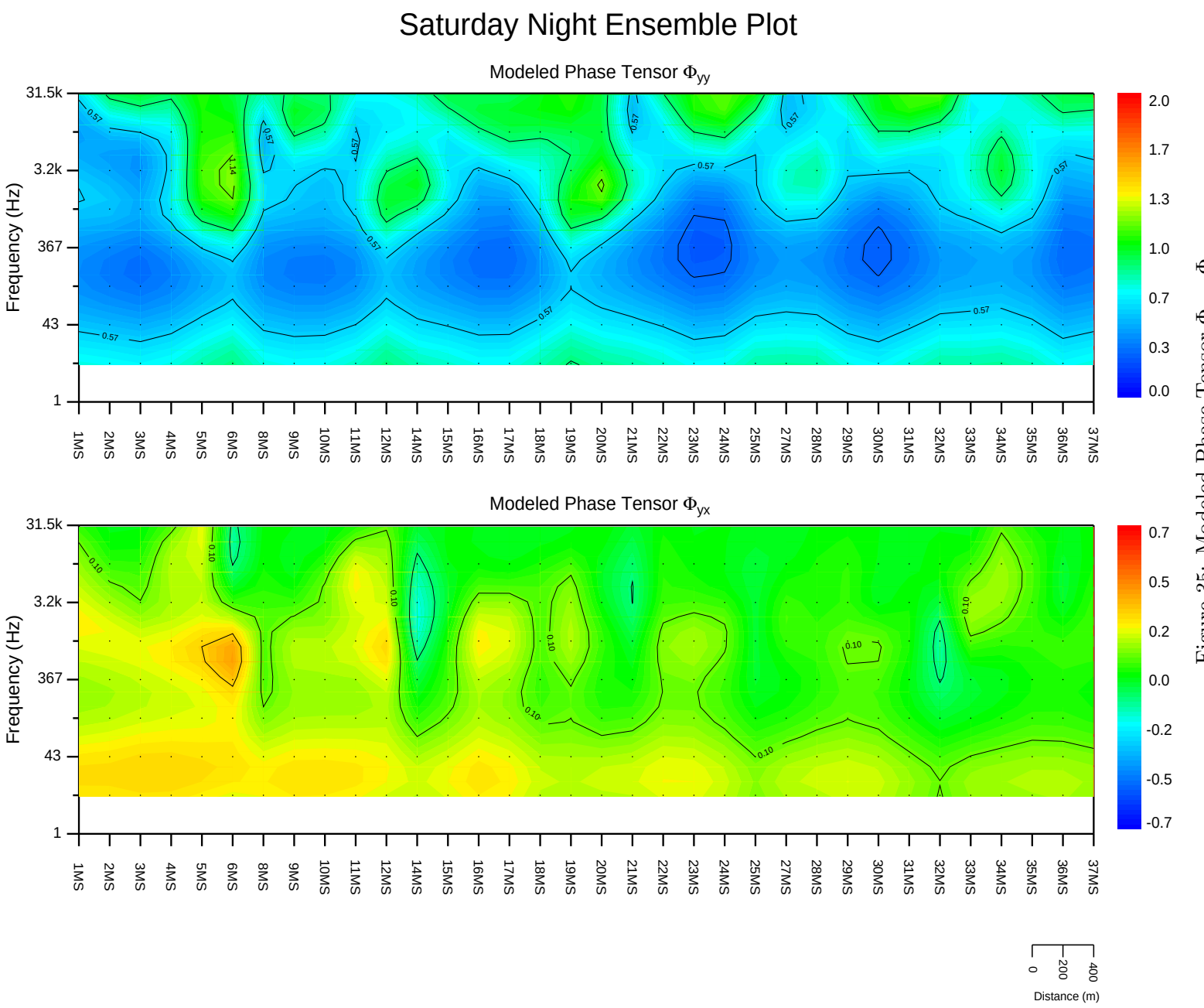

Figure 35: Modeled Phase Tensor Φ_{yx}, Φ_{yy}

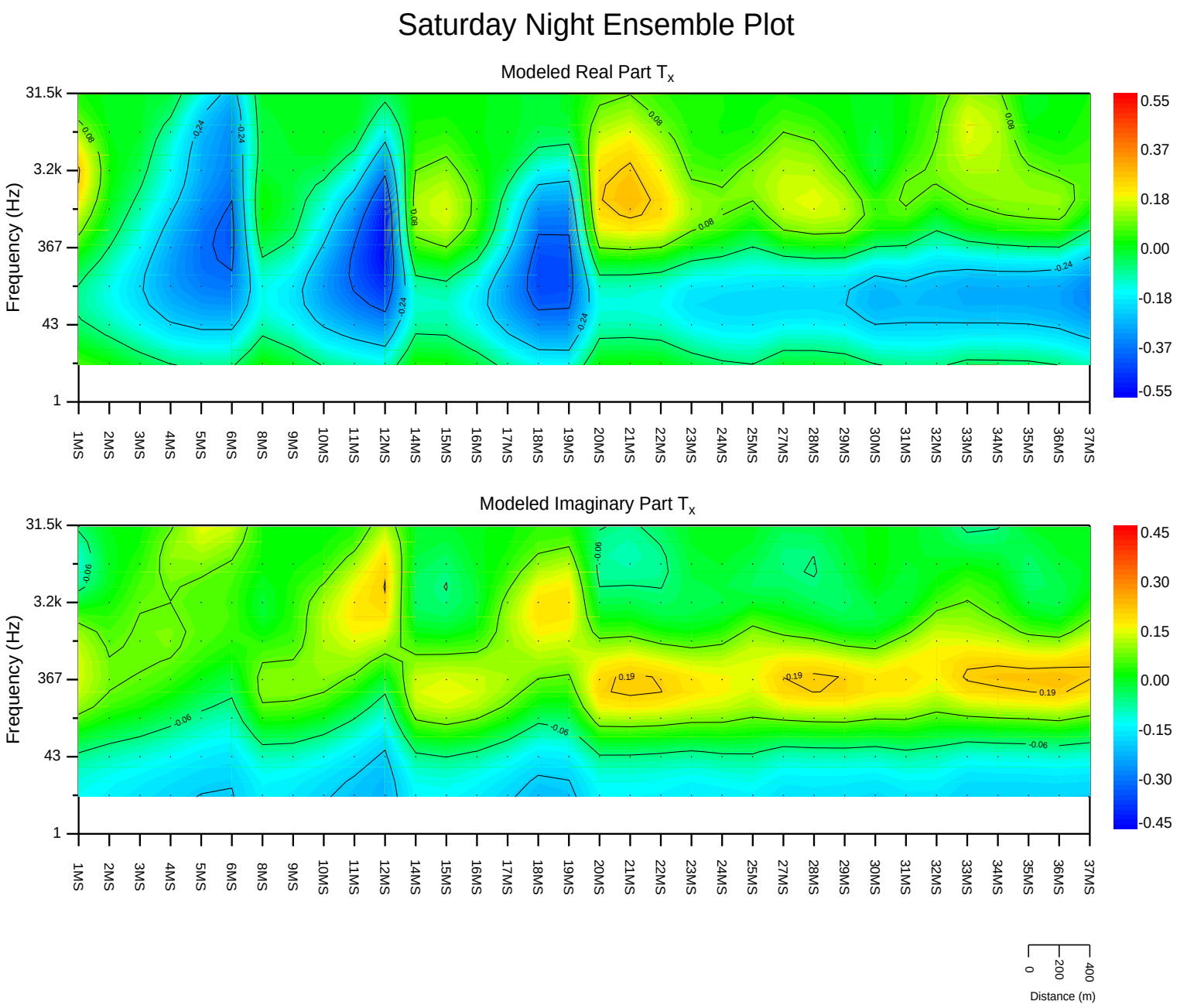

Figure 36: Modeled T_x

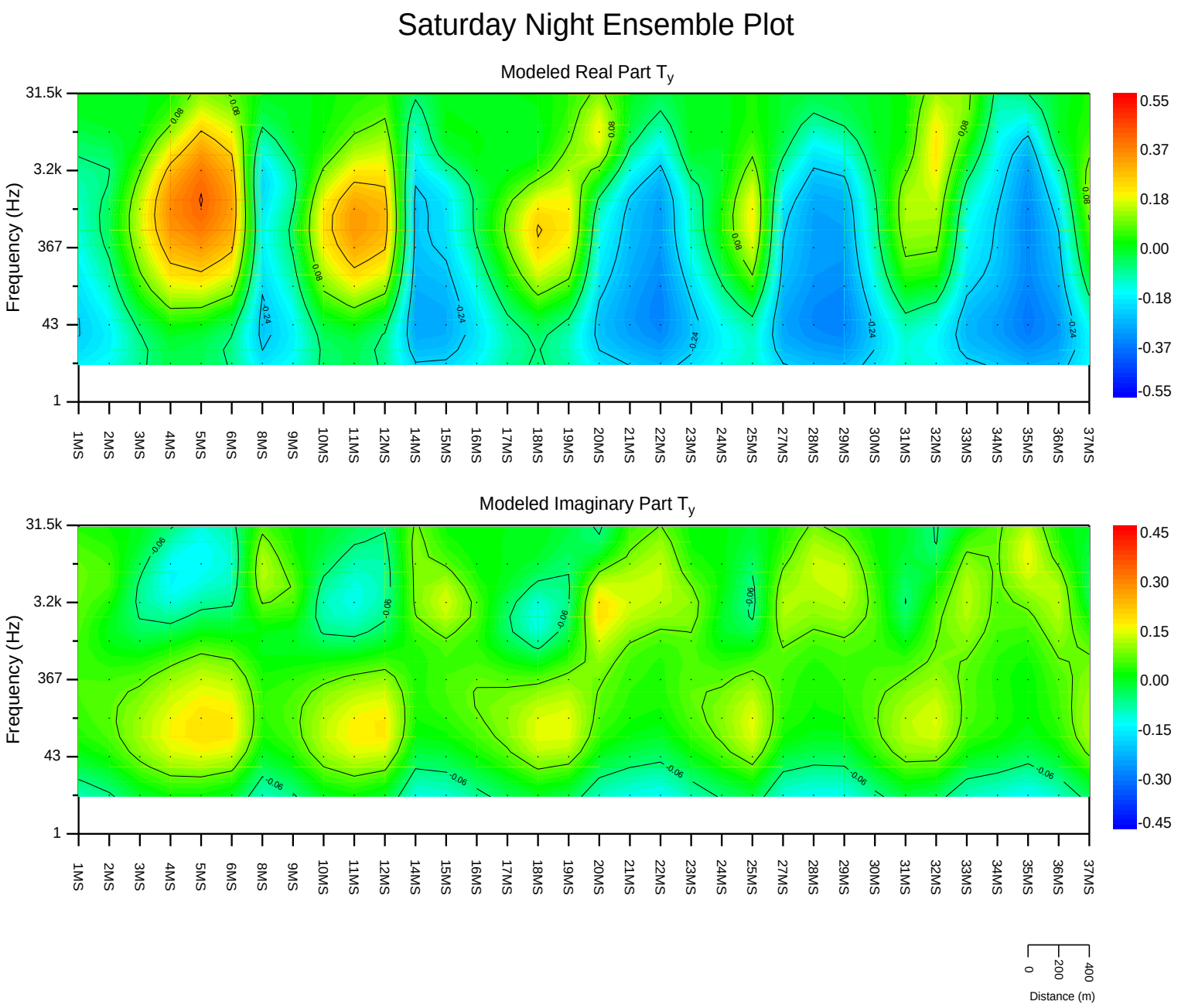

Figure 37: Modeled T_y

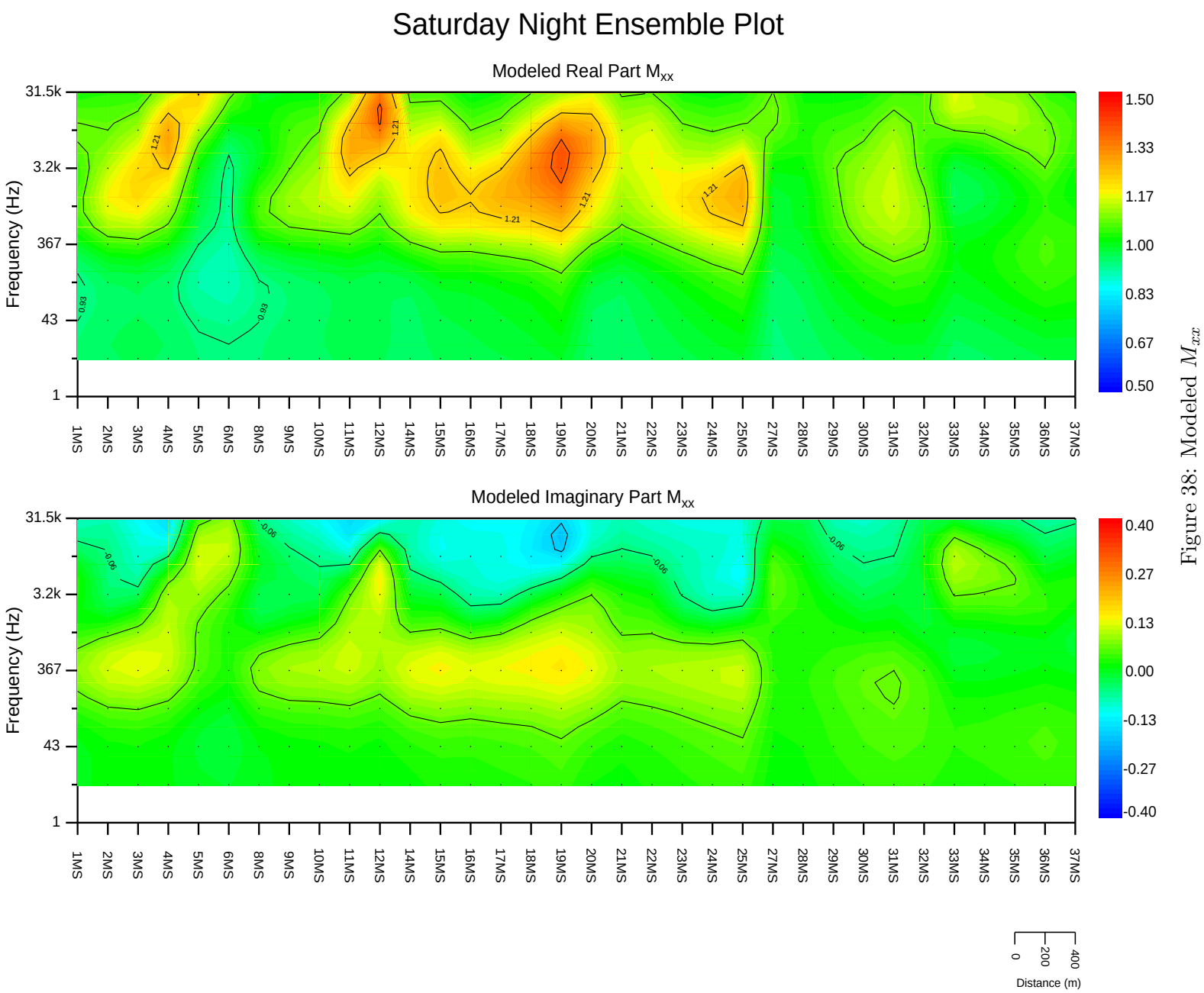

Figure 38: Modeled M_{xx}

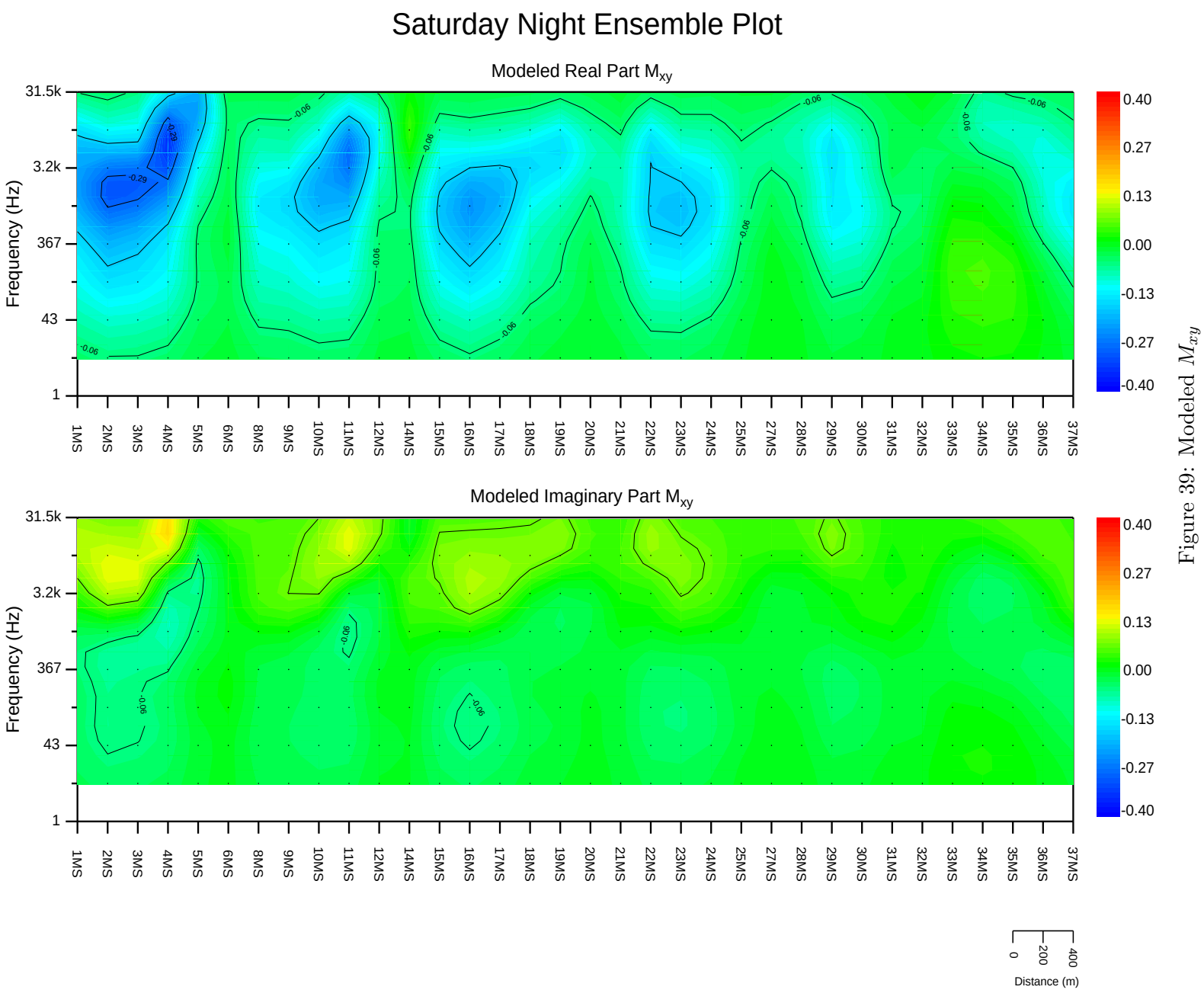

Figure 39: Modeled M_{xy}

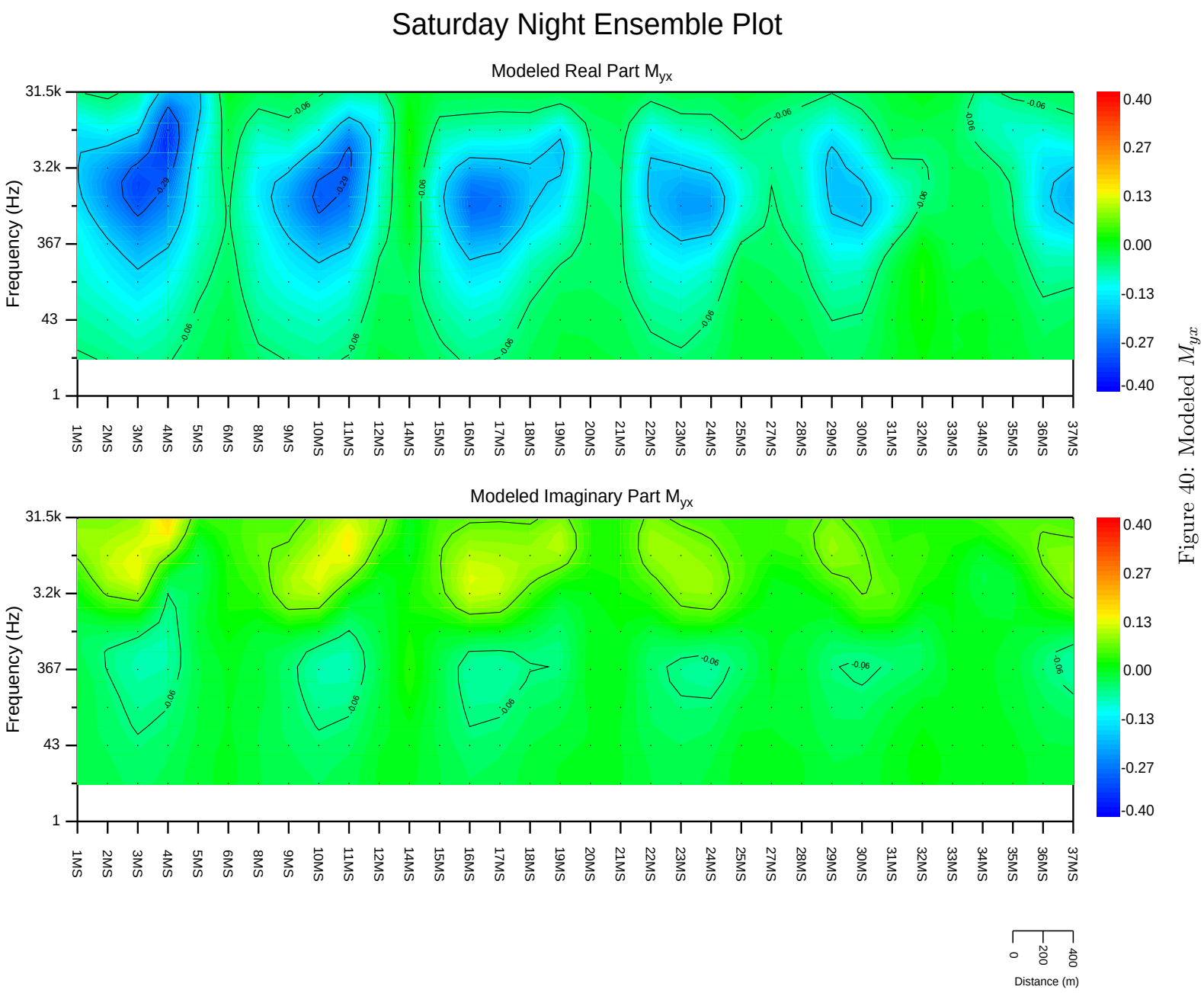

Figure 40: Modeled M_{yx}

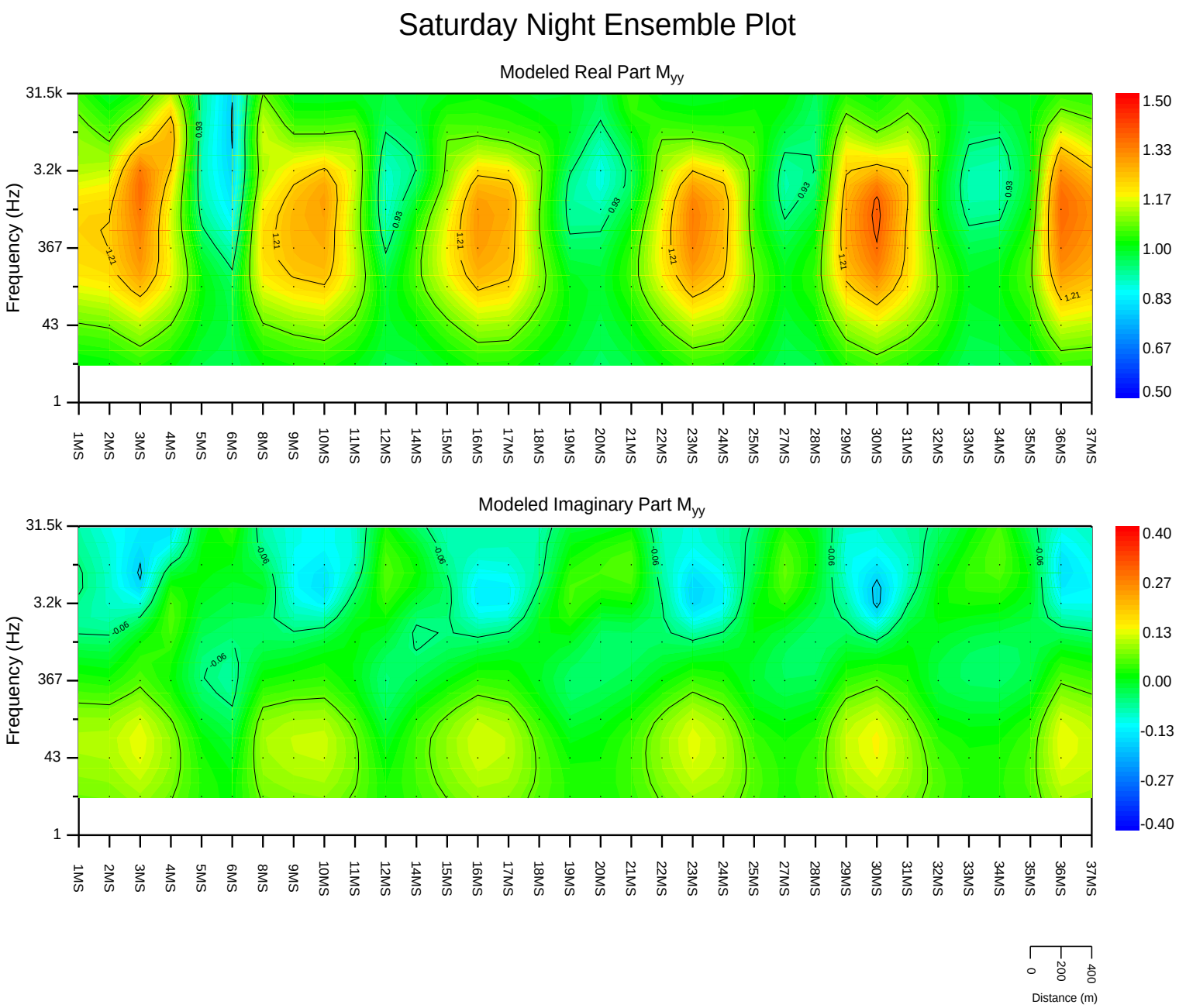

Figure 41: Modeled M_{yy}

4.3 Survey Logistics

Thirty-four impedance-tipper-magnetovariational PULSAR stations were collected at a spacing of $\approx$ 200 m in 6 survey days, average production was therefore 5.67 stations per day.

1. 04/08/18 - David Goldak, Andrew Schietzsch, Matthew Goldak and Dana Nesbitt leave Wawa 7:30 A.M., arrive Thunder Bay 1 P.M., check in to hotel, unpack and get out to property, access the property from the North without having to use Steve Ward's gate (he's never there), find a base station location.

2. 05/08/18 - Set up base station and work on the North part of the grid, we collect 4 stations and get "thundered-out" at our last station.

3. 06/08/18 - We get an okay start, leave McDonalds at 6:40 A.M. and get base station running by 7:20 A.M., we have an excellent day and collect 7 stations, was nice and cool in the morning and didn't get any warmer than 21 C, very little wind, no local thunderstorms, excellent day.

4. 07/08/18 - We continue to work on the North end of the grid and collect 6 stations, we finish the northern-most 3 lines, basically half done the survey, cold and foggy in the morning but then becomes quite warm in the afternoon.

5. 08/08/18 - We hike out to the West end of L1, and find that stations 1, 2 and 3 are in a swamp, lots of muskeg, spongy ground, we setup and collect our first station of the day, but during setup of the second station we get thundered out, at 10 A.M., will be a standby day.

6. 09/08/18 - We start with station 2 in the swamp and finish L1, then skip up to station 12 on L2 and station 19 on L3, excellent day, we collect 7 stations, no local lightning activity today.

7. 10/08/18 - Get a good start to the morning and hike out to the West end of L3, VERY humid today, we all sweat like crazy on the 1.2 km hike, despite the fact that it was nice and cool in the morning, collect 4 stations on L3 and then drop down to L2, was too swampy to collect the western-most station on L2 so we skip it, we collect 5 stations today and I call it a day as we watch a storm system steadily get closer through the day, in the morning it was about 500 km away and at our fifth station it was more like 300 km away, so I play it safe and call it quits for the day, and sure enough, by supper time it moves to within 50 km.

8. 11/08/18 - We work on stations 15 to 18 inclusive today, was VERY humid again, the bush was very wet as well, we all get soaked through and through, then becomes extremely hot in the afternoon, 32 C ambient when we shut down at 1:30 P.M., tear down base station, get back to hotel and pack up.

9. 12/08/18 - Leave Thunder Bay super early at 5 A.M. local time, will marathon drive it home, 17 hrs straight, we arrive into Saskatoon at 8 P.M. local time.

Withheld for client confidentiality.

Appendix B